MOLECULAR AND CELLULAR BIOLOGY, Nov. 2008, p. 6828–6843 Vol. 28, No. 22
0270-7306/08/$08.00+0 doi:10.1128/MCB.01297-08

Molecular Architecture of Quartet MOZ/MORF Histone Acetyltransferase Complexes▽§

Mukta Ullah,[1,2,3] Nadine Pelletier,[1,2] Lin Xiao,[1,2] Song Ping Zhao,[1] Kainan Wang,[1,3] Cindy Degerny,[1,2] Soroush Tahmasebi,[1,2] Christelle Cayrou,[4] Yannick Doyon,[4] Siew-Lee Goh,[1] Nathalie Champagne,[1] Jacques Côté,[4] and Xiang-Jiao Yang[1,2,3]*

Department of Medicine, McGill University Health Centre,[1] McGill Cancer Centre,[2] and Department of Biochemistry,[3] McGill University, Montréal, Québec, Canada, and Laval University Cancer Research Center, Hôtel-Dieu de Quebec (CHUQ), Québec City, Québec, Canada[4]

Received 14 August 2008/Accepted 8 September 2008

The monocytic leukemia zinc finger protein MOZ and the related factor MORF form tetrameric complexes with ING5 (inhibitor of growth 5), EAF6 (Esa1-associated factor 6 ortholog), and the bromodomain-PHD finger protein BRPF1, -2, or -3. To gain new insights into the structure, function, and regulation of these complexes, we reconstituted them and performed various molecular analyses. We found that BRPF proteins bridge the association of MOZ and MORF with ING5 and EAF6. An N-terminal region of BRPF1 interacts with the acetyltransferases; the enhancer of polycomb (EPc) homology domain in the middle part binds to ING5 and EAF6. The association of BRPF1 with EAF6 is weak, but ING5 increases the affinity. These three proteins form a trimeric core that is conserved from *Drosophila melanogaster* to humans, although authentic orthologs of MOZ and MORF are absent in invertebrates. Deletion mapping studies revealed that the acetyltransferase domain of MOZ/MORF is sufficient for BRPF1 interaction. At the functional level, complex formation with BRPF1 and ING5 drastically stimulates the activity of the acetyltransferase domain in acetylation of nucleosomal histone H3 and free histones H3 and H4. An unstructured 18-residue region at the C-terminal end of the catalytic domain is required for BRPF1 interaction and may function as an "activation lid." Furthermore, BRPF1 enhances the transcriptional potential of MOZ and a leukemic MOZ-TIF2 fusion protein. These findings thus indicate that BRPF proteins play a key role in assembling and activating MOZ/MORF acetyltransferase complexes.

The gene of MOZ (*mo*nocytic leukemia *z*inc finger protein, also referred to as MYST3 and KAT6A), located on chromosome 8p11, was first identified as a fusion partner in chromosome translocation t(8;16)(p11;p13) (2, 52). This recurrent translocation is associated with a monocytic subtype of acute myeloid leukemia and results in the fusion of the MOZ N-terminal domain to the C-terminal part of the transcription coactivator CBP. Two other leukemia-associated chromosomal rearrangements lead to the expression of proteins fusing MOZ fragments to the CBP paralog p300 and the p300/CBP-interacting nuclear receptor coactivator TIF2 (*t*ranscription *i*ntermediary *f*actor 2, also known as steroid receptor coactivator 2 [SRC-2] and nuclear receptor coactivator 2 [NCOA2]) (6, 8, 29, 34). One of the resulting fusion proteins, MOZ-TIF2, is known to promote self-renewal of leukemic stem cells (17, 25), suggesting that the chromosome abnormalities play a causal role in leukemogenesis. In addition, it was recently reported that MOZ is fused to NCOA3 (22), a TIF2 paralog synonymous with SRC-3 and AIB1 (*a*mplified *i*n *b*reast cancer 1). MOZ is highly homologous to MORF (*MOZ-r*elated *f*actors, also named Querkopf, MYST4, and KAT6B) (11, 64). The *MORF* gene is rearranged in leukemia patients with t(10;16)(q22;p13) (46) and in leiomyoma cases with t(10;17)(p11;q21) (40). The *CBP* gene is the fusion partner in the former translocation, while the *GCN5* gene is a potential candidate in the latter translocation. All of these findings suggest that deregulated acetylation has an important role in oncogenesis. In addition, recent studies indicate that MOZ and MORF play key roles in hematopoiesis, skeletogenesis, neurogenesis, and other developmental processes (16, 26, 38, 39, 62, 64). Therefore, MOZ and MORF are intimately linked to both normal development and cancer development (63, 69).

At the molecular level, available data suggest that this pair of paralogs functions as transcriptional coactivators with intrinsic histone acetyltransferase (HAT) activity (3, 11, 12, 27, 28, 48). Both possess the MYST domain, a catalytic core conserved among members of the MYST family of acetyltransferases (2, 52). Within this family, there are five members in humans, with the other three being TIP60, HBO1, and hMOF (1, 30, 51, 56). Although histones have been considered to be the major substrates, two recent studies show that in response to DNA damage, TIP60 and hMOF acetylate p53 at lysine 120 within the DNA-binding domain (59, 60). Moreover, DNA damage promotes TIP60 acetylation of ATM, upregulating the kinase activity (57). MOZ and MORF display similarities to the closest *Drosophila* protein Enok (*enok*i mushroom) only in the MYST domain and N-terminal part (53, 69), so unlike the other three mammalian MYST proteins, MOZ and MORF do not have authentic orthologs in *Drosophila* flies. The MYST

* Corresponding author. Mailing address: McGill Cancer Centre, Cancer Pavilion, Room 408, 1160 Pine Avenue West, Montréal, Québec H3G 0B1, Canada. Phone: (514) 398-5883. Fax: (514) 398-6769. E-mail: xiang-jiao.yang@mcgill.ca.

§ Supplemental material for this article may be found at http://mcb.asm.org/.

▽ Published ahead of print on 15 September 2008.

domain often remains intact in fusion proteins expressed from the aforementioned chromosome translocations (68), but the significance remains elusive. Known target DNA-binding transcription factors of MOZ and MORF include Runx proteins (3, 27, 28, 48), PU.1 (26), Nrf2-MafK (44), and perhaps peroxisome proliferator-activated receptor α (58). Available evidence suggests that MOZ and MORF control related pathological and developmental processes by acetylating histones and other proteins, but additional studies are needed to elucidate the underlying molecular mechanisms.

We have recently identified MOZ and MORF to be catalytic subunits of ING5 complexes (18), which reiterates that HATs often form multisubunit complexes in vivo (32, 43). ING5 is the fifth member of the novel ING (*in*hibitor of *g*rowth) tumor suppressor family (55). The other subunits of the MOZ/MORF complexes are EAF6 (homolog of yeast *E*sa1-*a*ssociated *f*actor 6) and BRPF1, -2, or -3 (*br*omodomain-*P*HD *f*inger protein 1, 2, or 3). BRPF1 and BRPF2 are also known as BR140 (*br*omodomain protein of *140* kDa) and BRD1 (*br*omo*d*omain protein 1), respectively (37, 65). By using an analogy to the Esa1 and TIP60 complexes (19), we postulated that different subunits of MOZ/MORF complexes regulate the acetyltransferase activity (18). To test this hypothesis, we carried out complex reconstitution and detailed molecular analysis. Here we present evidence that BRPF1 binds to the MYST domains of MOZ and MORF, stimulates acetyltransferase and coactivator activities, and bridges interaction with ING5 and EAF6. These results not only provide novel insights into the pathological and developmental processes involving MOZ, MORF, and associated subunits, but also shed light on regulation of the acetyltransferase activity in other MYST protein complexes.

MATERIALS AND METHODS

Plasmids and baculoviruses. Expression constructs for MOZ and MORF mutants were engineered from pcDNA3.1-Flag, a derivative of pcDNA3.1 (Invitrogen). Expression plasmids for full-length and deletion mutants of BRPF1, ING5, and EAF6 were subcloned into pcDNA3.1-Flag or pcDNA3.1-HA. The mutants were generated by PCR with Expand thermostable DNA polymerase (Roche). Baculovirus shuttle vectors were created by insertion of the coding sequences of BRPF1 proteins, ING5, and EAF6 into a pAcSG2-based vector for expression of hemagglutinin (HA)-tagged proteins. Linearized BaculoGold viral DNA (BD Biosciences) was used for generation of recombinant baculoviruses. The baculovirus for the MORF mutant H361 (Flag tagged) was described previously (11), and the virus for the MOZ mutant H810 (also Flag tagged) was generated on a pAcSG2-based vector for expression of Flag-tagged proteins in Sf9 cells. Expression plasmids for maltose-binding protein (MBP) fusion proteins were prepared from pMAL-C_2 (New England Biolabs), and green fluorescent protein (GFP) constructs were derived from pEGFP-C2 (BD Biosciences). Gal4 fusion constructs were prepared using a vector expressing the N-terminal 147 residues of the yeast Gal4 DNA-binding domain as described previously (11).

Generation and purification of polyclonal antibodies. The HAT domain of MORF was expressed as an MBP fusion protein and affinity purified on amylose resin as described previously (47). The purified fusion protein was dialyzed extensively against phosphate-buffered saline (PBS) and used for immunization of two rabbits. Antisera were subjected to affinity purification on CNBr-activated Sepharose 4 Fast Flow resins (GE Life Sciences) conjugated with the fusion protein. The HAT domain of MORF is almost identical to the corresponding region of MOZ (11), so the antibody recognizes both proteins. BRPF1, BRPF3, and ING5 antibodies were similarly generated except that full-length ING5 and the N-terminal 295 and 194 residues BRPF1 and BRPF3, respectively, were expressed as MBP fusion proteins and affinity purified on CNBr-activated Sepharose 4 Fast Flow resins conjugated with the respective fusion proteins.

Protein expression in and affinity purification from HEK293 cells. To examine protein interaction in HEK293 cells, 10 μg of expression plasmids was transfected into 5×10^5 to 10×10^5 cells (in a 10-cm dish) with 20 μl of the SuperFect transfection reagent (Qiagen). Forty-eight hours posttransfection, cells were washed twice with PBS and lysed in situ on ice in 1.0 ml cold buffer K150 (20 mM sodium phosphate [pH 7.0], 0.15 M KCl, 30 mM sodium pyrophosphate, 0.1% NP-40, 5 mM EDTA, 10 mM NaF, 0.1 mM Na_3VO_4, 2 μg/ml pepstatin A, 2 μg/ml aprotinin, 2 μg/ml leupeptin, and 1 mM phenylmethylsulfonyl fluoride). Soluble extracts were used for affinity purification on anti-Flag M2 agarose beads (Sigma). After being washed four times with 0.3 ml buffer K150 in a cold room, bound proteins were eluted in the same buffer containing Flag peptide (0.2 mg/ml). Eluted proteins were resolved by sodium dodecyl sulfate-polyacrylamide gel electrophoresis (SDS-PAGE) and transferred to a nitrocellulose membrane for immunoblotting with anti-Flag and anti-HA antibodies. Blots were developed with the SuperSignal West Pico substrate (Pierce).

Immunoprecipitation of endogenous proteins. Five or six 15-cm dishes of nearly confluent HEK293, WI-38, and NIH 3T3 cells were washed three times with PBS and used for isolation of nuclei as described previously (66). Nuclei were resuspended in 2.5 ml of cold buffer N150 (the same as for buffer K150 except that NaCl was used instead of KCl and the NP-40 concentration was 0.15%), transferred to two 1.5-ml tubes, and sonicated on ice for 10 s per tube with a Virsonic 100 sonicator (setting 5; VirTis). After being rotated at 4°C for 30 min, soluble extracts were collected by centrifugation for preclearing incubation with 100 μl protein A-Sepharose (GE Life Sciences) per tube. With further rotation at 4°C for 3 h, the slurry was centrifuged at 15,000 rpm for 5 min at 4°C with an Eppendorf microcentrifuge. The supernatants were carefully collected, and the centrifugation was repeated. The precleared extract was equally divided into six aliquots for immunoprecipitation with 0.6 μg goat anti-ING5 (Abcam) and anti-β-TRCP (Santa Cruz Biotechnology) polyclonal antibodies or with a similar amount of rabbit anti-MORF, anti-BRPF1, anti-BRPF3, and anti-GFP (Santa Cruz Biotechnology) antibodies. Protein A- or G-Sepharose beads (20 μl; GE Life Sciences) were added to tubes containing rabbit or goat polyclonal antibody, respectively. After rotation at 4°C for 14 to 18 h, the beads were washed once with 0.5 ml of buffer N150 and three times with buffer N300 (same as N150 except the NaCl concentration was 300 mM). Bound proteins were resolved by SDS-PAGE (8% or 10%) for immunoblotting with rabbit anti-MORF, anti-BRPF1, anti-BRPF3, and anti-ING5 antibodies. PBS containing 0.15% Tween 20 and 5% low-fat milk powder was used as the blocking and antibody incubation buffers. Incubation with the primary antibodies and the secondary antibody was carried out for 14 to 18 h at 4°C and 1 h at room temperature, respectively. After extensive washing, blots were developed with the SuperSignal West Femto maximum sensitivity chemiluminescent substrate (Pierce).

Protein interaction in vitro. Radiolabeled BRPF1 or deletion mutants were synthesized in the presence of [^{35}S]methionine using a TNT T7-coupled in vitro transcription and translation kit (Promega). For binding assays, bacterial extracts containing MBP fusion proteins were incubated in 20 μl amylose resin for 30 min at 4°C (with rotation). The resin was washed twice in buffer K150 and used for incubation with in vitro synthesized products. After rotation at 4°C for 1 h, the beads were washed four times with buffer K and used for elution with the same buffer containing 10% maltose. Eluted proteins were separated by SDS-PAGE for autoradiography.

Reconstitution of MOZ and MORF complexes in Sf9 insect cells. Sf9 cells were maintained at 27°C as suspension culture in spinner flasks (Bellco) as described previously (47). For small-scale expression or complex reconstitution, exponentially growing cells were added to 10-cm tissue culture dishes, about 7×10^6 cells per dish, to achieve 90 to 95% confluence after attaching. The dishes were incubated at 27°C for 1 h to allow the cells to attach. The dishes were then transferred back to a tissue culture hood for virus addition. For complex reconstitution, the baculovirus for Flag-H361 or Flag-H810 was used to coinfect the cells along with viruses for HA-tagged BRPF1, ING5, and/or EAF6. For analysis of BRPF1 domains, viruses for deletion mutants were used to replace those for full-length BRPF1. Forty to 48 h postinfection, dishes were scraped and cell suspension was collected in 15-ml Falcon tubes for centrifugation (~2,500 × *g* at room temperature for 5 min). About 10 ml of PBS was used to resuspend and wash each cell pellet, which was then resuspended in 1 ml PBS and transferred to a 1.5-ml Eppendorf tube. After centrifugation at ~2,500 × *g* and room temperature for 5 min, the resulting pellet was resuspended in 1 ml cold buffer N150 and sonicated on ice for 10 s using a Virsonic 100 sonicator (setting 5; VirTis). After rotation at 4°C for 30 min and centrifugation, soluble extracts were collected and incubated with 20 μl of anti-Flag M2 agarose beads (Sigma), which were pretreated with 0.1 M glycine-HCl (pH 2.5) for 4 to 5 min, neutralized with 0.1 M Tris-HCl (pH 7.5 to 8.0), and preequilibrated with buffer N150. After rotation at 4°C for 2 to 4 h, the beads were collected by brief centrifugation at 4°C and washed once with 0.5 ml of buffer N150 and three times with buffer N300 in a cold room. Washed beads were mixed with 30 μl of buffer N150 containing Flag

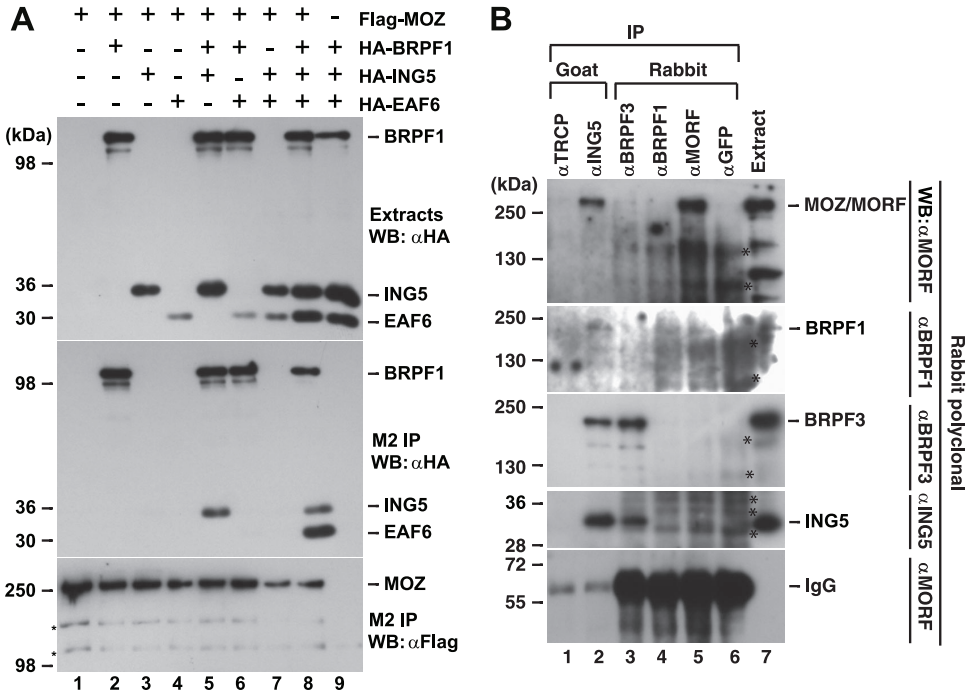

FIG. 1. Interaction of MOZ and MORF with BRPFs, ING5, and EAF6 in vivo. (A) The expression plasmid for Flag-MOZ was transfected into HEK293 cells along with those for HA-tagged BRPF1, ING5, and EAF6 as specified. Extracts were prepared in buffer K150 for affinity purification on M2 agarose, and bound proteins were eluted with Flag peptide for subsequent Western blotting (WB) with anti-HA (αHA) and anti-Flag (αFlag) monoclonal antibodies. The asterisks denote degraded MOZ fragments. (B) Nuclear extracts were prepared from HEK293 cells for immunoprecipitation with goat and rabbit anti-MORF (αMORF), anti-ING5 (αING5), anti-BRPF1 (αBRPF1), and anti-BRPF3 (αBRPF3) polyclonal antibodies as indicated at the top, with the goat anti-β-TRCP and rabbit anti-GFP antibodies as the negative controls. Precipitated proteins were resolved by SDS-PAGE (10% for detection of ING5 and 8% for MOZ/MORF, BRPF1, and BRPF3). For immunoblotting, rabbit anti-MORF, anti-BRPF1, anti-BRPF3, and anti-ING5 polyclonal antibodies were used as shown on the right. Between the two anti-ING5 antibodies, the goat antibody is more efficient for immunoprecipitation (especially coimmunoprecipiation of MOZ/MORF, BRPF1, and BRPF3) and the rabbit antibody is more specific for immunoblotting. The anti-MORF antibody also recognizes MOZ. As the control, extracts (~1% of the input for one immunoprecipitation) were loaded on lanes 7. Nonspecific bands are marked with asterisk at their right. Compared to the goat anti-ING5 antibody, the anti-MORF, anti-BRPF1, and anti-BRPF3 antibodies were less efficient in coimmunoprecipitation, perhaps because the epitopes for the antibodies are masked in the complexes and the antibodies destabilize the complexes (the antigens encompass the sites required for complex formation; see Materials and Methods). IgG H, immunoglobulin G heavy chain.

peptide (0.4 mg/ml). After rotation at 4°C for 1 h, the eluate was collected by brief centrifugation at 4°C and flash-frozen in aliquots on dry ice. For analysis of purity and complex composition, 2 to 5 μl of the eluate was resolved by SDS-PAGE (10%) and stained overnight with "blue silver" (5), prepared from Coomassie colloidal blue G-250.

HAT assays and substrate preparation. HAT activity determination was carried out as described previously (47), except that a 10-min incubation at 30°C was used for oligonucleosomes. MOZ and MORF proteins were affinity purified from Sf9 cells in buffer N150 for acetylation of histone octamers and oligonucleosomes, which were prepared from nuclei of HeLa S3 cells essentially as reported previously (15).

Indirect immunofluorescence and live green fluorescence microscopy. For indirect fluorescence microscopic analysis, NIH 3T3 cells were seeded at 2×10^4 cells per well on flamed glass coverslips in 12-well tissue culture plates. The SuperFect transfection reagent (Qiagen) was used to transfect the cells, and indirect immunofluorescence microscopy was performed as described previously (23). For live green fluorescence microscopy, HEK293 cells were seeded at 4×10^4 cells per well in 12-well tissue culture plates and transfected with expression plasmids for GFP or its fusion proteins. Eighteen hours posttransfection, green fluorescence of live cells was examined under an Axiovert 135 microscope (Zeiss), which was linked to a Regia CCD camera. An imaging system from the QImaging Corporation was used to control the camera for image capture. Image files were further processed with Adobe Photoshop and Illustrator.

Reporter gene assays. Reporter gene assays were performed as described previously (23, 48). The luciferase (Luc) reporter constructs 6OSE2-Luc, OG2-Luc, and GM-CSF-Luc have been described previously (14, 48). For internal control, a cytomegalovirus immediate early promoter-driven β-galactosidase expression plasmid was cotransfected. D-(−)-Luciferin (Boehringer Mannheim) and Galacto-Light Plus (Tropix) were utilized as substrates for luciferase and β-galactosidase, respectively. Chemiluminescence from these substrates was measured on 96-well plates by a FLUOstar Optima luminometer (BMG Labtech). The resulting data were directly copied for Excel calculation, and the calculated results were transferred for statistical analysis and graph generation with GraphPad Prism 5.

RESULTS

Interaction of MOZ and MORF with BRPFs, ING5, and EAF6. To gain further insight into the molecular anatomy of MOZ and MORF complexes (18), we first carried out coimmunoprecipitation to analyze the interaction of Flag-MOZ with HA-tagged BRPF1, ING5, and EAF6. As shown in Fig. 1A, MOZ coprecipitated BRPF1 but not ING5 or EAF6 (lanes 1 to 4). Coexpression of BRPF1, however, promoted association of ING5 with MOZ (Fig. 1A, compare lanes 3 and 5), supporting the view that BRPF1 bridges the interaction between MOZ and ING5 (18). In contrast, expression of BRPF1 or ING5 had minimal effects on EAF6 association with MOZ (Fig. 1A, compare lanes 4, 6, and 7). When both ING5 and BRPF1 were expressed, EAF6 copurified efficiently with MOZ

(Fig. 1A, lanes 8 to 9), indicating that the presence of both ING5 and BRPF1 is essential for tetrameric complex formation. Moreover, coexpression of these two proteins appeared to stabilize EAF6 (Fig. 1A, compare lanes 4 and 6 to 9, top panel). These results indicate that BRPF proteins play a key role in assembling tetrameric complexes containing MOZ and MORF.

We also analyzed interaction of endogenous proteins using polyclonal antibodies against MOZ/MORF, BRPF1, BRPF3, and ING5 (antibodies against BRPF2 and EAF6 were not yet available). For this, nuclear extracts were prepared from HEK293 cells for immunoprecipitation. As shown in Fig. 1B, the goat anti-ING5 polyclonal antibody, but not the goat anti-β-TRCP antibody, efficiently precipitated endogenous ING5 (compare lanes 1, 2, and 7, bottom two panels). Importantly, immunoblotting with the respective antibodies detected MOZ/MORF, BRPF1, and BRPF3 in the immunoprecipitate from the anti-ING5 antibody but not that from the anti-β-TRCP antibody (Fig. 1B, lanes 1, 2, and 7, top three panels), indicating that endogenous ING5 interacts with endogenous MOZ/MORF, BRPF1, and BRPF3. Consistent with this, the anti-BRPF3 but not the anti-GFP antibody coprecipitated ING5 (Fig. 1B, compare lanes 3, 6, and 7, bottom three panels). MOZ/MORF was also detected in the immunoprecipitate from the anti-BRPF3 antibody (Fig. 1B, lane 3, top panel). In addition, BRPF1 appeared to be present in the anti-MORF immunoprecipitate (Fig. 1B, compare lanes 4 to 5, top two panels). Some of these interactions could also be detected in WI38 and NIH 3T3 fibroblasts (data not shown). Together, these findings strongly support the view that ING5 forms complexes with MOZ, MORF, and BRPF proteins in vivo.

Subcellular localization of MOZ and the noncatalytic subunits of its complex. Next we examined subcellular localization of the proteins involved. For this, HA-BRPF1 was expressed alone or with other subunits for analysis of subcellular localization by fluorescence microscopy. When expressed alone in NIH 3T3 cells, HA-BRPF1 was mainly cytoplasmic, accumulating in dot-like structures (Fig. 2A). When MOZ was coexpressed, BRPF1 was found exclusively in the nucleus (Fig. 2B). As reported previously (27, 28), MOZ was mainly nuclear (Fig. 2C), so the change of BRPF1 subcellular localization suggests that MOZ promotes nuclear localization of BRPF1. Similar to MOZ, both ING5 and EAF6 promoted the nuclear localization of BRPF1 (Fig. 2D to E). These results are consistent with the physical association of these four proteins.

We also expressed GFP-BRPF1 in HEK293 cells and analyzed effects of expression of MOZ, ING5, and EAF6 by live green fluorescence microscopy. As in NIH 3T3 cells, GFP-BRPF1 formed cytoplasmic dots in HEK293 cells (see Fig. S1A in the supplemental material). While the effect of MOZ expression was less dramatic in these cells than that in NIH 3T3 cells (data not shown), ING5 expression promoted BRPF1 translocation to the nucleus, where it formed dots (see Fig. S1A in the supplemental material). Expression of EAF6 alone had minimal impact, but upon coexpression of both ING5 and EAF6, BRPF1 became exclusively nuclear (see Fig. S1A in the supplemental material). GFP-ING5 was pannuclear or showed nucleolar accumulation in some cells; when BRPF1 was coexpressed, GFP-ING5 became enriched in nuclear dots (see Fig. S1B in the supplemental material). GFP-EAF6 localized to nucleoli in the majority of cells, but when both BRPF1 and ING5 were coexpressed, this fusion protein accumulated in nuclear dots (see Fig. S1C in the supplemental material). These results indicate that BRPF1, ING5, and EAF6 localize to nuclear dots when they are expressed together, providing further support for their physical association.

Mapping the BRPF1-binding domains of MOZ and MORF. To locate the minimal domains of MOZ and MORF required for BRPF1 binding, we first analyzed three mutants of MOZ (N352, N760, and C1409) (Fig. 3A) and three mutants of MORF (N716, C1238, and H424) by coimmunoprecipitation. As shown in Fig. 3B, BRPF1, ING5, and EAF6 coprecipitated with N716 and H424, but not with the other four mutants, indicating that the MYST domain is responsible and sufficient for complex formation. To substantiate this, we expressed different MORF mutants as MBP fusion proteins in *Escherichia coli* and performed in vitro binding assays. These assays revealed that BRPF1 interacts with mutant H361, but not with N359, C1564, or C1567 (Fig. 3A and C), supporting direct interaction of the MYST domain with BRPF1. Moreover, the MYST domain of MOZ or MORF interacts similarly with different BRPF proteins in vitro (see Fig. S2A in the supplemental material). To determine how the MYST domain may interact with BRPF1, we analyzed mutants H361, H553, and H460 (Fig. 3A) by in vitro binding assays. As shown in Fig. 3D, these three mutants were all able to bind BRPF1, indicating that the binding does not require residues 424 to 459 and 553 to 588, regions corresponding to the C2HC finger and the acetyl coenzyme A (acetyl-CoA) binding motif, respectively (11).

It was unexpected that the MOZ mutant N760 failed to form a complex with BRPF1, ING5, and EAF6 (Fig. 3A and B). The MYST domain is highly conserved in MOZ, and mutant N760 contains almost the entire MYST domain except residues 761 to 810, so we considered whether this small region is critical for complex formation. To address this, we expressed mutants H810, H760, and H783 (Fig. 3A) as MBP fusion proteins in *E. coli* for in vitro binding assays. Mutants H810 and H783 but not H760 were able to bind BRPF1 (Fig. 3E), indicating that residues 761 to 782 are essential for binding. This is in agreement with the inability of mutant H760 to form a tetrameric complex with BRPF1, ING5, and EAF6 in HEK293 cells (Fig. 3A to B). We also affinity purified the MBP fusion proteins and compared their HAT activities. As reported previously (11, 12), mutant H810 was active in acetylating free histones (Fig. 3F). In comparison, H783 had 20% of the activity, whereas H760 was totally inactive (Fig. 3F), indicating that residues 761 to 782 are crucial for HAT activity. Interestingly, this region is conserved between MOZ and MORF but more divergent in other MYST proteins (see Fig. S2B in the supplemental material) (2, 52, 67). At the structural level, it is located right next to the catalytic center (see Fig. S2C in the supplemental material) (24, 67), so this region has an important role in modulating acetyltransferase activation.

Locating the MOZ/MORF-binding sites of BRPF1. To determine how BRPF1 bridges the association of ING5 and EAF6 with MOZ or MORF, we first mapped the MOZ/MORF-binding site on BRPF1. For this, deletion mutants BR1, BR2, and BR3 (Fig. 4A) were expressed as HA-tagged fusion proteins in HEK293 cells along with Flag-tagged H361,

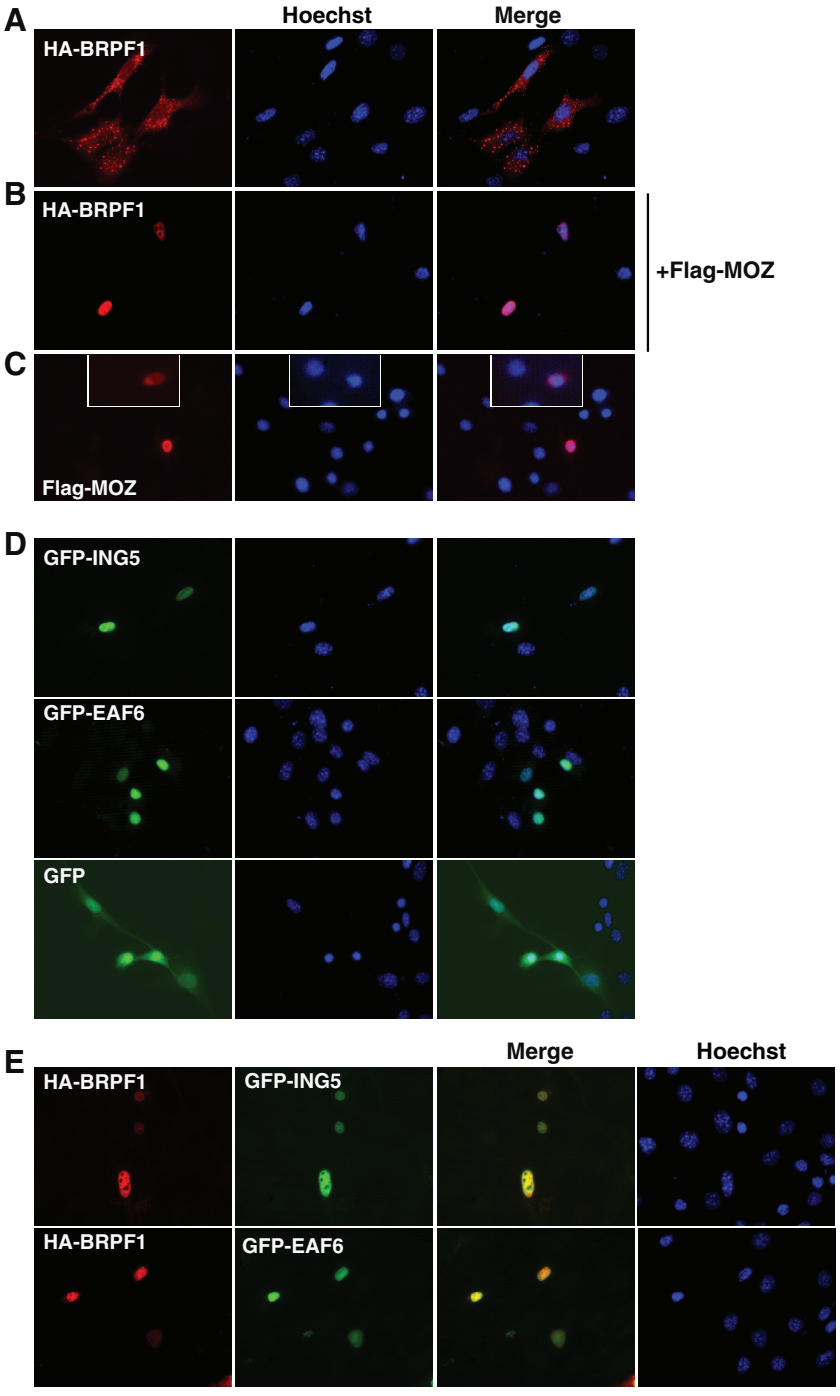

FIG. 2. Subcellular localization of BRPF1, ING5, and EAF6. (A, B) The expression plasmid for HA-BRPF1 was transfected into NIH 3T3 cells with (+Flag-MOZ) or without the Flag-MOZ expression plasmid. BRPF1 expression was detected by immunostaining with anti-HA antibody and a Cy3-labeled secondary antibody. Unlike BRPF1, both BRPF2 and BPRF3 were mainly nuclear (data not shown). (C) The expression plasmid for Flag-MOZ was transfected into NIH 3T3 cells. Expression of Flag-MOZ was detected by immunostaining with anti-Flag antibody and a Cy3-labeled secondary antibody. (D) The expression plasmid for GFP-ING5, GFP-EAF6, or GFP was transfected into NIH 3T3 cells. After fixation, GFP signals were analyzed by green fluorescence microscopy. (E) The expression plasmid for HA-BRPF1 was transfected into NIH 3T3 cells along with that for GFP-ING5 (top) or GFP-EAF6 (bottom). HA-BRPF1 was detected by immunostaining with anti-HA antibody and the Cy3-labeled secondary antibody, whereas localization of GFP fusion proteins was determined by green fluorescence microscopy.

a MORF mutant able to bind BRPF1 (Fig. 3A). Cell extracts were prepared for affinity purification on M2 agarose, and bound proteins were eluted with Flag peptide for immunoblotting with anti-Flag and anti-HA antibodies. As shown in Fig. 4B, mutant BR1 coprecipitated with H361 as efficiently as full-length BRPF1 (lanes 1 to 2). Mutant BR2 was much less efficient, and BR3 was unable to do so (Fig. 4B, lanes 3 and 4). These results suggest that BRPF1 contains two MORF-binding

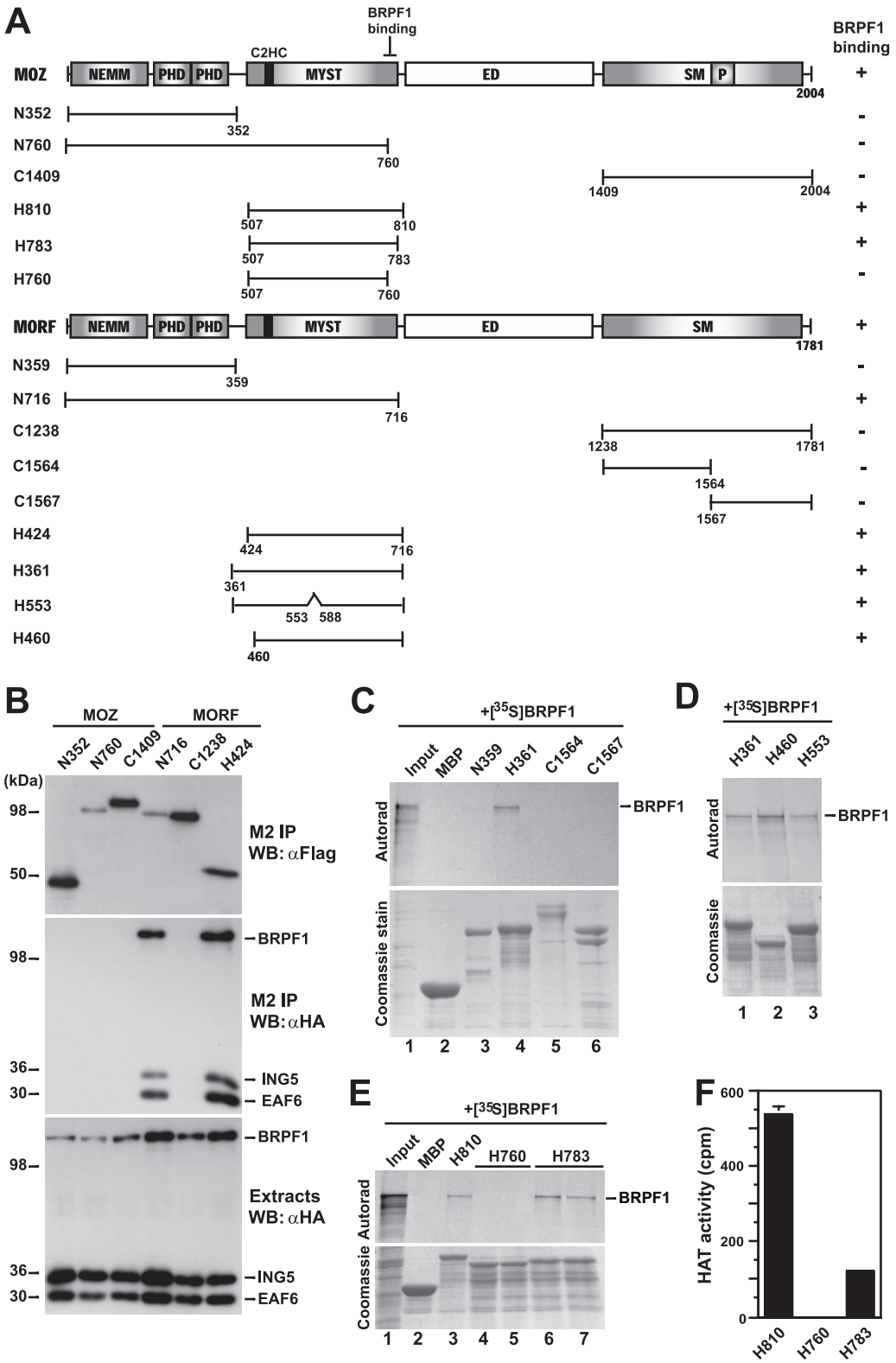

FIG. 3. Mapping the BRPF1-binding site on MOZ and MORF. (A) Schematic representation of MOZ, MORF, and their deletion mutants, with the BRPF1-binding ability summarized on the right. Domains are labeled as follows: NEMM, N-terminal part of Enok, MOZ, or MORF; PHD, PHD zinc finger; ED, glutamate/aspartate-rich region; SM, serine/methionine-rich region; and P, proline/glutamine stretch. (B) Expression plasmids for HA-BRPF1, HA-ING5, and HA-EAF6 were cotransfected into HEK293 cells along with the construct for a Flag-tagged MOZ or MORF deletion mutant (N352, N760, C1409, N716, C1238, or H424). Extracts were prepared for affinity purification on M2 agarose, and bound proteins were eluted with Flag peptide for immunoblotting with anti-HA and anti-Flag antibodies. (C to E) The indicated MOZ/MORF mutants were expressed as MBP fusion proteins for immobilization on amylose agarose and subsequent incubation with [^{35}S]methionine-labeled BRPF1 (+[^{35}S]BRPF1). After extensive washing, bound proteins were eluted and analyzed by SDS-PAGE and Coomassie blue staining. The gels were dried for autoradiography. The input lanes represent 20% of [^{35}S]methionine-labeled BRPF1 used for one binding assay. (F) Equal amounts of MBP fusion proteins, expressed in and affinity purified from bacteria, were subjected to HAT activity determination using mixed free histones (calf thymus; Sigma) as the substrates.

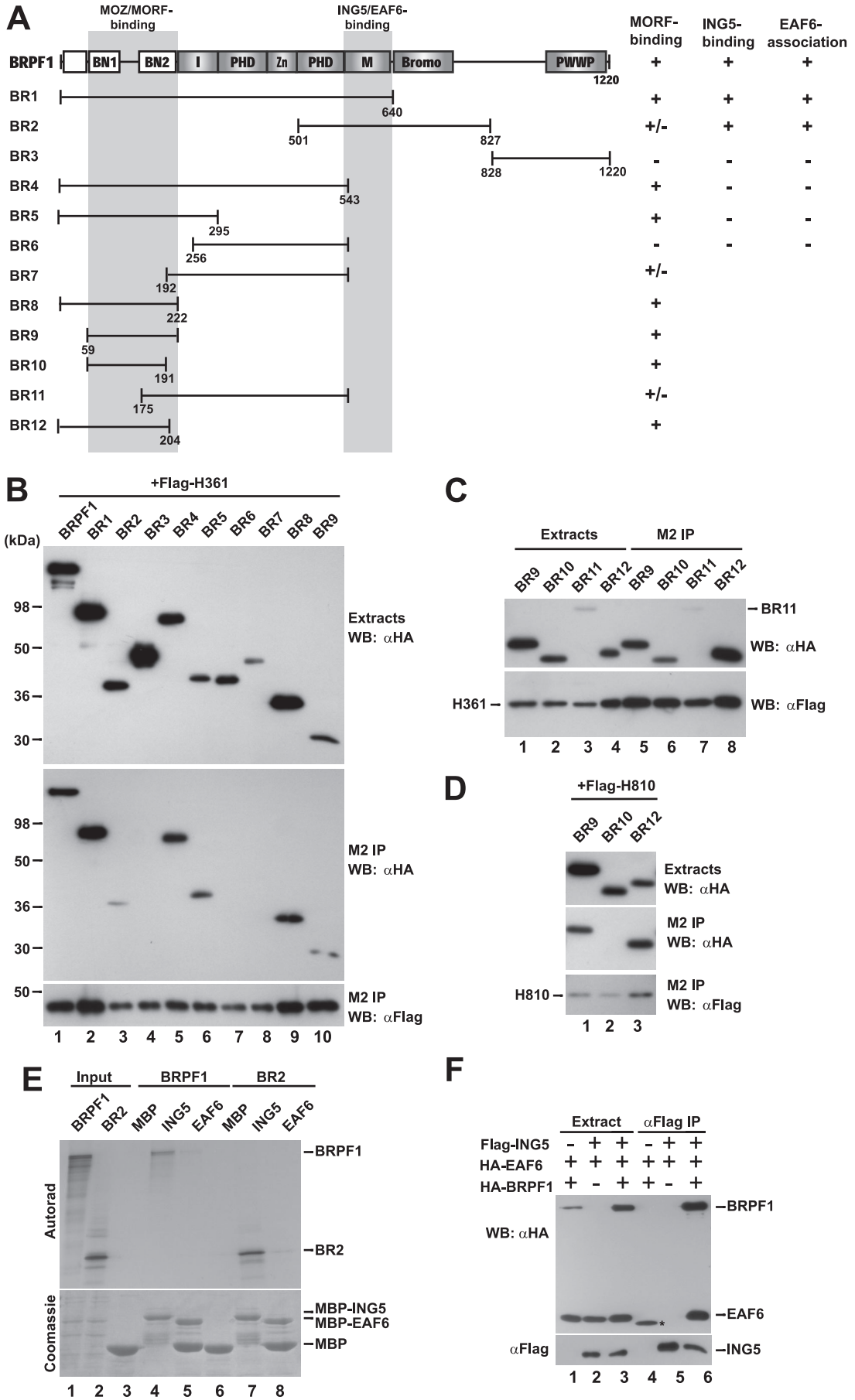
A
MOZ/MORF-binding
ING5/EAF6-binding
MORF-binding
ING5-binding
EAF6-association
BRPF1
BN1
BN2
I
PHD
Zn
PHD
M
Bromo
PWWP
1220
BR1
640
BR2
501
827
BR3
828
1220
BR4
543
BR5
295
BR6
256
BR7
192
BR8
222
BR9
59
BR10
191
BR11
175
BR12
204
B
+Flag-H361
BRPF1 BR1 BR2 BR3 BR4 BR5 BR6 BR7 BR8 BR9
(kDa)
98
50
36
30
Extracts
WB: αHA
M2 IP
WB: αHA
M2 IP
WB: αFlag
1 2 3 4 5 6 7 8 9 10
C
Extracts
M2 IP
BR9 BR10 BR11 BR12 BR9 BR10 BR11 BR12
BR11
WB: αHA
H361
WB: αFlag
1 2 3 4 5 6 7 8
D
+Flag-H810
BR9 BR10 BR12
Extracts
WB: αHA
M2 IP
WB: αHA
H810
M2 IP
WB: αFlag
1 2 3
E
Input
BRPF1
BR2
BRPF1 BR2 MBP ING5 EAF6 MBP ING5 EAF6
Autorad
Coomassie
BRPF1
BR2
MBP-ING5
MBP-EAF6
MBP
1 2 3 4 5 6 7 8
F
Extract
αFlag IP
Flag-ING5 - + + - + +
HA-EAF6 + + + + + +
HA-BRPF1 + - + + - +
WB: αHA
BRPF1
EAF6
αFlag
ING5
1 2 3 4 5 6

sites, with a strong one located within the N-terminal region and a weak one in the middle. To delineate the strong binding site, we analyzed six other mutants, BR4 to BR9 (Fig. 4B). Among them, BR4, BR5, BR8, and BR9 coprecipitated with H361 (Fig. 4B, lanes 5 to 10), indicating that the binding site encompasses residues 59 to 222 of BRPF1 (Fig. 4A).

To map the binding site further, we performed a multiple-sequence analysis of known BRPF proteins. This analysis revealed that BRPF proteins are conserved from *Caenorhabditis elegans* to humans (see Fig. S3A in the supplemental material). From the analysis, it became clear that residues 59 to 222 of BRPF1 possess two conserved subdomains, BN1 (BRPF N-terminal conserved region 1) and BN2 (see Fig. S3B in the supplemental material). Based on this, we generated three more mutants, BR10, BR11, and BR12 (Fig. 4A; see Fig. S3B in the supplemental material). Mutant BR10 interacted with H361 only slightly less efficiently than BR9 (Fig. 4C, compare lanes 1 to 2 and 5 to 6). In coprecipitation with H361, mutant BR12 was at least as efficient as BR9 (Fig. 4C, compare lanes 1, 4, 5, and 8). Unlike BR7 (Fig. 4A and B), mutant BR11 coprecipitated with H361 (Fig. 4C, lanes 3 and 7), albeit less efficiently than BR9. These results indicate that the BN2 subdomain is important for MORF binding. We also analyzed the interaction of BR9, BR10, and BR12 with the MOZ mutant H810, which is equivalent to H361 (Fig. 3A). Surprisingly, mutant BR10 was unable to bind H810 (Fig. 4D). This finding is unexpected and supports the idea that the BN2 subdomain is even more important for MOZ interaction. Together, the above results indicate that the BN2 subdomain, and perhaps also the BN1 subdomain, form the binding site for MOZ/MORF (Fig. 4A).

To substantiate this, we performed in vitro binding assays. For this, mutant H361 was expressed as an MBP fusion protein to pull down [^{35}S]methionine-labeled BRPF1 and mutants. As shown in Fig. S4A in the supplemental material, BRPF1, BR1, BR5, and BR8, but not BR3 or BR7, associated with MBP-H361, supporting evidence that the BN1 and BN2 subdomains mediate direct interaction with MOZ and MORF (Fig. 4A).

Mapping the ING5- and EAF6-binding sites on BRPF1. We then performed coimmunoprecipitation to determine which domain of BRPF1 interacts with ING5. ING5 interacted with BRPF1, BR1, and BR2, but not with BR3, BR4, BR5, or BR6 (see Fig. S4B in the supplemental material), indicating that domain M mediates the interaction (Fig. 4A). Similarly, the EAF6-binding site was mapped to the same region (see Fig. S4C in the supplemental material). We also analyzed the interaction of ING5 and Eaf6 with BRPF1 using in vitro binding assays. MBP-ING5 associated efficiently with BRPF1 and BR2 in vitro (Fig. 4E, lanes 1 to 4 and 6 to 7). In contrast, the interaction of MBP-EAF6 with BRPF1 was undetectable (Fig. 4E, lanes 5 and 8). Coimmunoprecipitation experiments suggested that ING5 may stabilize the interaction of EAF6 with MOZ (Fig. 1A), and EAF6 precipitated with BRPF1 when they were overexpressed in HEK293 cells (see Fig. S4C in the supplemental material), so we examined whether ING5 binds to EAF6 directly. As shown in Fig. 4F, ING5 could not form a stable complex with EAF6, but the presence of BRPF1 promoted formation of a trimeric complex. This is consistent with the finding from live green fluorescence microscopy that BPRF1 forms a trimeric complex with ING5 and EAF6 (see Fig. S1 in the supplemental material). Therefore, different regions of BRPF1 mediate interaction with MOZ/MORF, ING5, and EAF6 (Fig. 4A).

Effect of BRPF1, ING5, and EAF6 on the HAT activity of MOZ/MORF. We subsequently investigated how the associated subunits affect the HAT activity of MOZ and MORF. To analyze this systematically, we generated recombinant baculoviruses expressing these subunits. Given the observation that the MYST domain of MOZ/MORF is sufficient for BRPF1 binding (Fig. 3A), we employed the baculovirus for Flag-H361 to assemble complexes in Sf9 cells. Different combinations of baculoviruses for HA-BRPF1, HA-ING5, and HA-EAF6 were used to coinfect Sf9 cells with that for Flag-H361. Proteins were affinity purified on M2 agarose and analyzed by colloidal blue staining (Fig. 5A). HA-BRPF1 copurified with Flag-H361 to an almost stoichiometric level (Fig. 5A, lanes 1 to 2), further supporting the view that the interaction is specific. HA-ING5 did not efficiently copurify with Flag-H361 unless HA-BRPF1 was present (Fig. 5A, lanes 3 and 5), confirming that the interaction of ING5 with MORF is indirect. HA-EAF6 copurified with Flag-H361 only when both HA-ING5 and HA-BRPF1 were present (Fig. 5A, lanes 4 and 6). Similar results were obtained with Flag-tagged H810 (Fig. 5B), the mutant corresponding to the MYST domain of MOZ (Fig. 3A). In addition, mutant BR1, but not BR4 or BR5, was capable of forming the tetrameric complex with H361 (Fig. 5C) and H810 (data not shown). Together, these results are consistent with the mapping data described above (Fig. 4A) and provide strong support for the conclusion that BRPF1 plays a scaffolding role in complex formation.

We then compared HAT activities of the reconstituted complexes. BRPF1 drastically increased the activity of the MORF

FIG. 4. Delineation of MOZ/MORF-, ING5-, and EAF6-binding sites of BRPF1. (A) Schematic representation of BRPF1 and deletion mutants, with numbers indicating positions of the N- or C-terminal residues. MORF-, ING5-, and EAF6-binding abilities are summarized on the right. Domains of BRPF1 are labeled as follows: BN, BRPF1 N-terminal domain; I and M, the N- and C-terminal halves of the Epc homology domain, respectively; PHD, PHD finger; Zn, monoknuckle zinc finger; bromo, bromodomain; and PWWP, conserved proline-tryptophan-tryptophan-proline domain. (B, C) Interaction of BRPF1 and mutants with the MYST domain of MORF. The expression vector for Flag-H361 (Fig. 3A) was transfected into HEK293 cells with expression plasmids for BRPF1 and mutants as indicated. Extracts were prepared for affinity purification on M2 agarose, and purified proteins were analyzed by immunoblotting with anti-HA and anti-Flag antibodies. The description for panel D is the same as that for panel C except that interaction of BR9, BR10, and BR12 with the MOZ mutant H810 (Fig. 3A) was analyzed. (E) BRPF1 associates with ING5 and EAF6 in vitro. Bacterial extracts expressing MBP, MBP-ING5, and MBP-EAF6 were incubated with amylose agarose in the presence of [^{35}S]methionine-labeled BRPF1 and BR2. Bound proteins were analyzed by SDS-PAGE, followed by Coomassie blue staining and autoradiography. (F) Interaction of ING5 with BRPF1 and EAF6 in vivo. HEK293 cells were transfected with expression plasmids for Flag-ING5, HA-EAF6, and HA-BRPF1 as indicated. Extracts were prepared for immunoprecipitation on M2 agarose and immunoblotting with anti-HA and anti-Flag antibodies. An asterisk (lane 4, top panel) denotes the residual immunoglobulin G light chain.

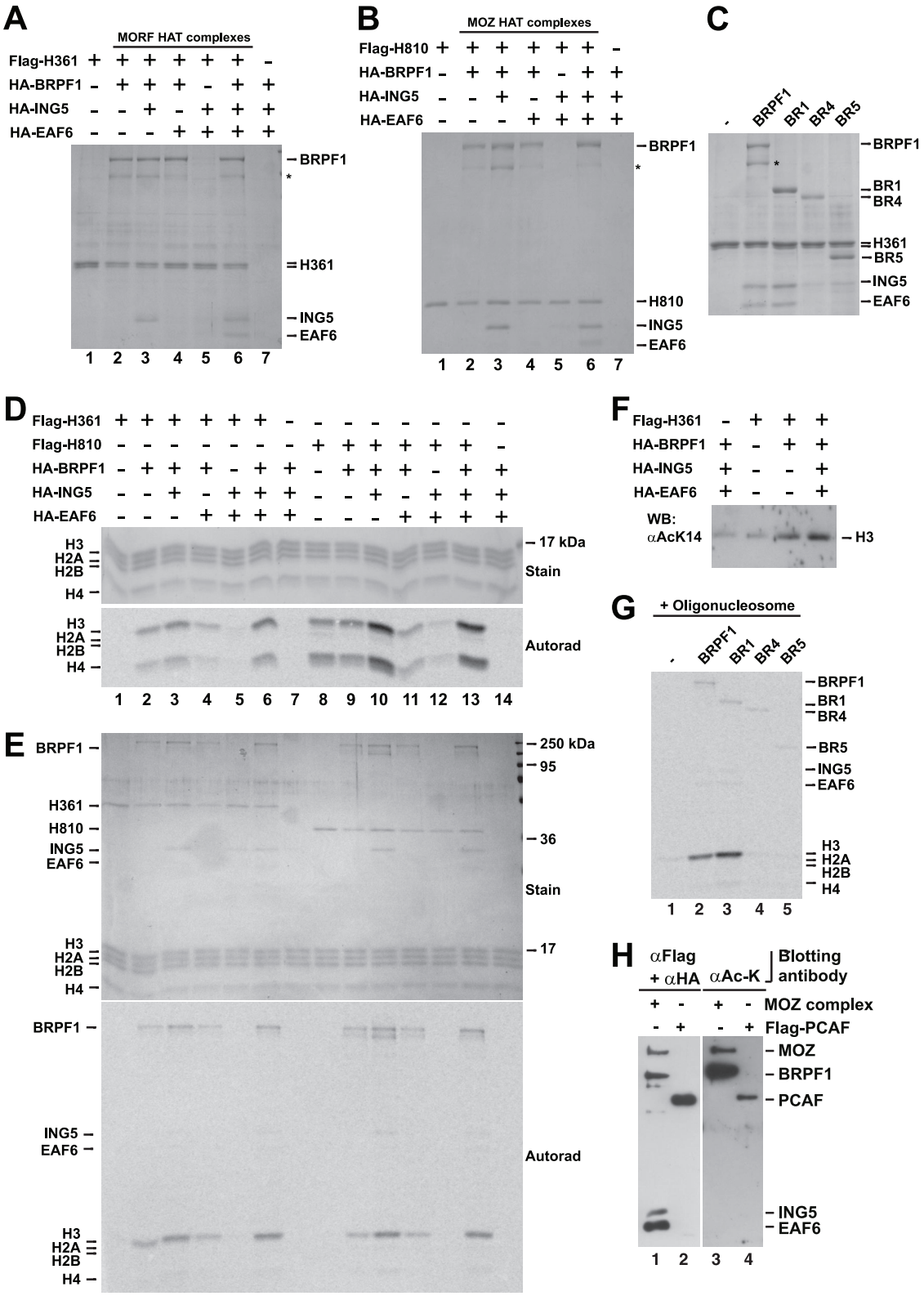

FIG. 5. Reconstitution and characterization of MOZ and MORF complexes. (A, B) Sf9 insect cells were infected with the baculovirus for Flag-H361 (A) or Flag-H810 (B) along with recombinant baculoviruses for HA-tagged BRPF1, ING5, and EAF6 as indicated. Extracts were prepared in buffer N150 for affinity purification on M2 agarose, and bound proteins were eluted with Flag peptide. Purified complexes were resolved by SDS-PAGE and detected by colloidal blue-derived "blue silver" staining. (C) Sf9 insect cells were infected with baculoviruses for Flag-H361 and HA-tagged ING5 and EAF6, along with recombinant baculoviruses for HA-tagged BRPF1 and mutants as indicated. Complexes were purified and analyzed as described for panel A. (D, E) HAT activity determination. Complexes reconstituted as described for panels A and

HAT domain toward free histones H3 and H4 (Fig. 5D, compare lanes 1 and 5 with lane 2). ING5 increased this activity further, while EAF6 had minimal effects (Fig. 5D, compare lanes 2 and 3 with lanes 4 and 6, respectively). With oligonucleosome as the substrate, only histone H3 was acetylated (Fig. 5E, lanes 1 to 7), indicating that substrate specificity changes when histones are presented in a different form. As with free histones H3 and H4, BRPF1 and ING5 stimulated the acetyltransferase activity of the MORF MYST domain toward nucleosomal histone H3. One acetylation site was lysine 14 (Fig. 5F), but lysines 9, 18, and 23 were not acetylated (data not shown). Consistent with the affinity for ING5, mutant BR1, but not BR4 and BR5, enhanced the ability of H361 to acetylate nucleosomal histone H3 (Fig. 5G). With free and nucleosomal histones, the MOZ mutant H810 exhibited similar responses to BRPF1 and ING5, although the effect of BRPF1 on free histones is less dramatic compared to the MORF HAT domain (Fig. 5D and E, lanes 8 to 14). These results indicate that both BRPF1 and ING5 activate the MYST domain to acetylate nucleosomal histone H3 and free histones H3 and H4.

The HAT assays also revealed that the MYST domain of MOZ or MORF acetylates BRPF1 (Fig. 5E). ING5 appeared to stimulate the acetylation (Fig. 5E, compare lane 3 with lanes 2 and 4 and also lane 10 with lanes 9 and 11). At least some of the acetylation sites were located at the region corresponding to mutant BR5 (Fig. 5G). Consistent with the results from in vitro assays, BRPF1 was acetylated in vivo (Fig. 5H). Further studies are needed to determine the functional consequence of BRPF1 acetylation. Notably, the mutants were acetylated to similar levels (compare Fig. 5C and G), indicating that domain M is essential for efficient acetylation of histones H3 and H4 but not so important for BRPF1 acetylation. Weak acetylation of ING5 and EAF6 was detectable in vitro (Fig. 5E, lanes 3, 6, 10, and 13, and G, lanes 2 and 3), but there is no evidence for this modification in vivo (Fig. 5H).

Effect of BRPF1, ING5, and EAF6 on transcriptional activation by MOZ. MOZ and MORF are known coactivators for the Runx family of transcription factors (3, 27, 28, 48), so we investigated how associated subunits might be involved. For this, reporter gene assays were performed with the reporter 6OSE2-Luc, which contains six copies of the Runx2-responsive element from the murine osteocalcin gene 2 promoter to drive the transcription of the luciferase gene (21, 48). As reported previously (18), BRPF1 synergized with full-length MOZ in potentiating Runx2-dependent transcription (Fig. 6A and B). This effect was dose dependent (data not shown). We also tested two other reporters, OG2-Luc and GM-CSF-Luc, under the control of 0.2- and 0.65-kb native fragments of murine osteocalcin gene 2 and granulocyte macrophage colony-stimulating factor (GM-CSF) promoters, respectively (14, 21, 48). Runx2 and Runx1 are known to activate OG-Luc and GM-CSF-Luc, respectively. As with 6OSE2-Luc, BRPF1 potentiated the activation of both promoters (Fig. 6C and D). We also analyzed G658E and C543G, two MOZ mutants known to inactivate the acetyltransferase activity and disrupt the C2HC zinc finger of the MYST domain, respectively (17). Neither mutant synergized with BRPF1 (Fig. 6A), indicating that both the acetyltransferase activity and the C2HC finger are important for functional interaction with BRPF1.

To delineate which domain of BRPF1 is required for synergizing with MOZ transcription, we analyzed various deletion mutants. As shown in Fig. 6B and in Fig. S5B in the supplemental material, mutants BR1 and BR4 were comparable to full-length BRPF1, whereas mutant BR13 was slightly more active, and the other mutants had minimal or inhibitory effects. Similar results were obtained with the reporter OG2-Luc (Fig. 6C). These results suggest that the region from the bromodomain to the N-terminal end of the PWWP domain is responsible for the synergizing effect on activation by MOZ (Fig. 6E). These results also indicate that the PWWP domain has a negative role. Consistent with this, mutant BR13 was more active than full-length BRPF1 when the reporter GM-CSF-Luc was used (Fig. 6D). With this reporter, mutants BR1, BR4, BR5, and BR9 were comparable to full-length BRPF1, but the other three mutants had minimal effects, suggesting the MOZ/MORF-interacting region is important for activation.

To determine if BRPF1 possesses a portable transacting domain, we investigated whether BRPF1 can activate transcription when tethered to a promoter by the Gal4 DNA-binding domain. Gal4-BRPF1 exhibited no activation potential (data not shown), supporting evidence that transcriptional stimulation by BRPF1 is context dependent.

In similar assays, Gal4-ING5 repressed reporter gene activity (data not shown). Related to the repressive effect of ING5, we found that coexpression of ING5 diminished the ability of BRPF1 to activate Runx2-dependent transcription of both 6OSE2-Luc and OG2-Luc (see Fig. S6A in the supplemental material). The effect on 6OSE2-Luc is different from what was previously observed (18); the reason for this discrepancy is unclear, even though we have made great efforts and investigated various possibilities. Different from these two reporters, the GM-CSF promoter activity was activated by ING5 (see Fig. S6B in the supplemental material), indicating that the effects are context dependent. Coexpression of EAF6 inhibited the

B were incubated with HeLa histone octamers (D) or oligonucleosomes (E) in the presence of [^{14}C]acetyl-CoA. Reaction mixtures were resolved by SDS-PAGE (15%) for "blue sliver" staining (top) and autoradiography (bottom). In the particular preparation used for the assay shown on lanes 1 to 7 (E), the NP-40 concentration in the purification buffers was 0.1% and ING5 appeared to associate with H361 (lane 5), but the band on this lane disappeared when the NP-40 concentration increased to 0.15%, indicating that the association is not specific. Note that about 50-fold-larger amounts of the enzymes were used for assays with nucleosome substrates. (F) MORF complexes were reconstituted as described for panel A for acetylation in the presence of regular acetyl-CoA. Reaction mixtures were resolved by SDS-PAGE for immunoblotting with anti-acetylated histone H3 antibodies specific to lysines 9, 14, 19, and 23. (G) Complexes were reconstituted as described for panel C and used for acetylation of oligonucleosomes as described for panel E. (H) Flag-MOZ was expressed in HEK293 cells along with HA-BRPF1, HA-ING5, and HA-EAF6. Extracts were prepared in buffer K150, supplemented with trichostatin A and nicotinamide, for affinity purification on M2 agarose. Purified proteins were immunoblotted with a mixture of anti-Flag and anti-HA antibodies (left) or with an acetyl-lysine antibody (right). As a control, Flag-PCAF was expressed, affinity purified, and analyzed similarly (lanes 2 and 4).

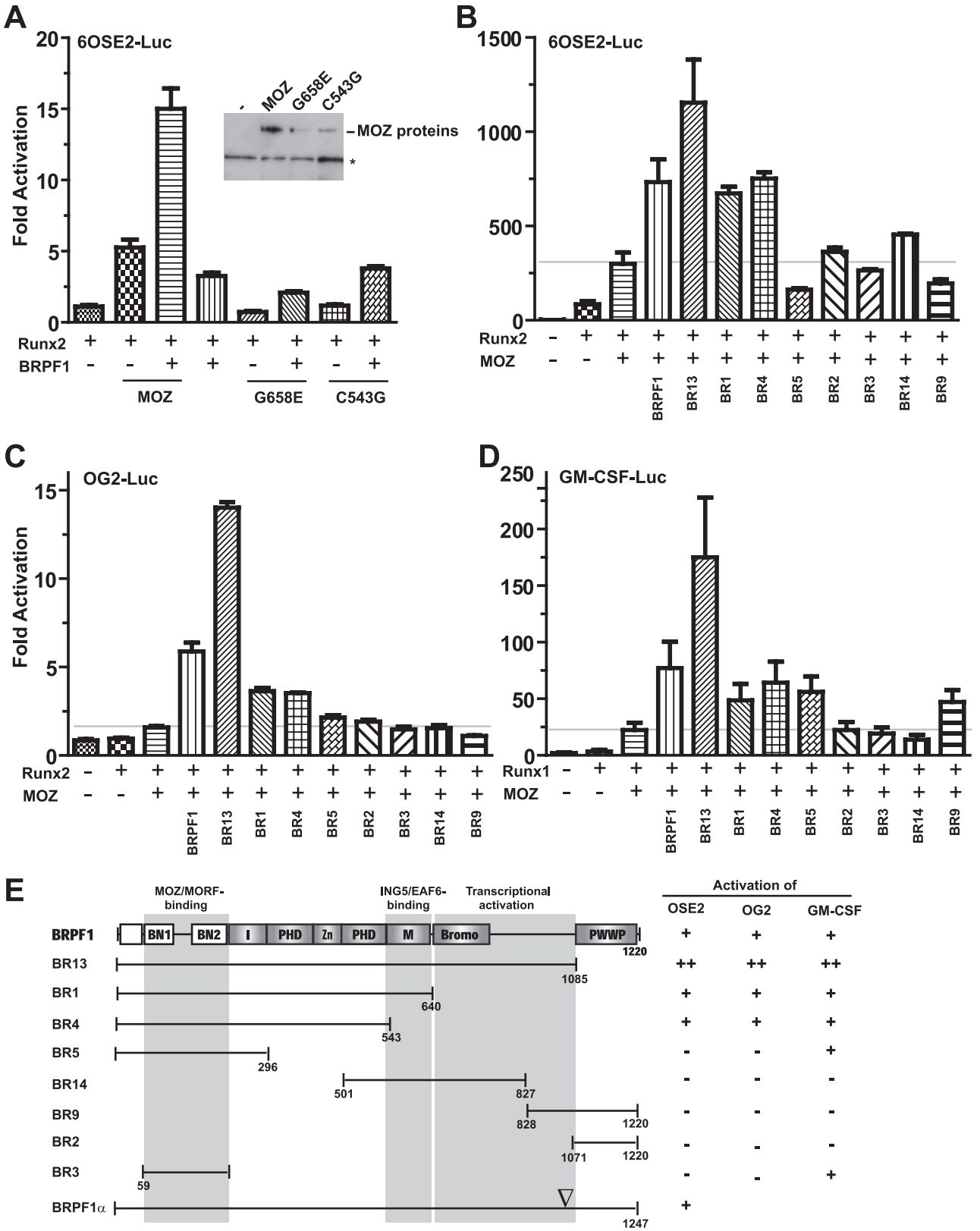

FIG. 6. Transcriptional coactivation by BRPF1 and mutants. (A) The 6OSE2-Luc reporter and a β-galactosidase reporter were cotransfected into HEK293 cells along with expression plasmids for Runx2 (0.05 μg), BRPF1 (0.2 μg), and MOZ (0.1 μg) or its point mutants (0.3 μg each) as indicated. Luciferase activities were measured and normalized against β-galactosidase activities. Normalized luciferase activity from the transfection with Runx2 was arbitrarily set to 1.0. In the insert, expression levels of MOZ and point mutants (all Flag tagged) were determined by immunoblotting with anti-Flag antibody, with an asterisk marking the position of nonspecific bands. (B) The expression plasmids for Runx2 (0.05

activities of all three reporters (data not shown). Further studies are needed to determine how ING5 and EAF6 regulate endogenous target genes.

Effect of BRPF1 on transcriptional regulation by MOZ-TIF2. Leukemia-associated chromosome translocations involving MOZ or MORF often express fusion proteins containing the intact MYST domain (68), but the significance remains unclear. Having established that this domain is sufficient for tetrameric complex formation with BRPF1, ING5, and EAF6 (Fig. 3), we asked whether the leukemic fusion proteins form similar complexes with these subunits. For this, coimmunoprecipitation was performed with MOZ-TIF2, a leukemic fusion protein able to promote stem cell renewal and regulate transcription (17, 25, 27). As shown in Fig. 7A, this fusion protein formed a tetrameric complex almost as efficiently as the wild-type MOZ. In addition, this fusion protein stimulated the activity of GM-CSF-Luc, and BRPF1 synergized with the fusion protein in the activation (Fig. 7B). The effect appeared to be specific to the GM-CSF promoter as minimal impact was observed with the reporter 6OSE2-Luc (Fig. 7C). Thus, BRPF1 interacts with MOZ-TIF2 and modulates its transcriptional potential.

DISCUSSION

A scaffold role of BRPF proteins in MOZ/MORF complexes. Reminiscent of p300 and CBP, MOZ and MORF form a pair of enzymatic transcriptional coactivators with important roles in leukemogenesis and normal developmental programs (63, 68). Compared to p300 and CBP, much less is known about MOZ and MORF. The recent identification of MOZ and MORF as catalytic subunits of quartet complexes provides an opportunity for studying how associated subunits may regulate the acetyltransferase activities and other functions of MOZ and MORF (18). The results presented herein indicate that BRPF proteins bridge the association of MOZ and MORF with ING5 and EAF6 (Fig. 1 and 2). The BN1 and BN2 subdomains of BRPF1 interact with the acetyltransferases (Fig. 4A and 8A; see Fig. S3 in the supplemental material), which is consistent with a very recent report that the N-terminal region of mouse BRPF1α (Fig. 6E; see Fig. S5B in the supplemental material) interacts with MOZ (31). Our data also show that an enhancer of polycomb (EPc) homology region, domain M, binds directly to ING5 and mediates association with EAF6 (Fig. 4A and 8A).

This molecular anatomy provides direct support for the hypothesis that the MOZ and MORF complexes are structurally analogous to the TIP60-ING3 core complex and the HBO1-ING4/5 complexes (18, 20). First, EAF6 is also present in TIP60-ING3 and HBO1-ING4/5 complexes, and yeast Eaf6 is a subunit of the NuA3 and NuA4 acetyltransferase complexes, both of which contain yeast ING proteins (7, 19). NuA3 and NuA4 are MYST acetyltransferase complexes possessing Sas3 and Esa1, respectively; Esa1 is the yeast ortholog of TIP60, and Sas3 displays some functional similarity to MOZ (1, 30). Second, BRPF1, BRPF2, and BRPF3 share domains I and M with EPc1, a subunit of the TIP60 complex (18, 20). These two small domains are homologous to an N-terminal region of *Drosophila* Epc and have been collectively referred to as Epc-N (50). They are also present in Jade (gene [*J*] for *a*poptosis and *d*ifferentiation in *e*pithelia) 1, 2, or 3, a subunit of HBO1-ING4/5 complexes (18). Finally, different from Epc proteins, each BRPF protein has two PHD fingers linked by a mononuclear zinc knuckle separating domains I and M. Together, the PHD fingers and the zinc knuckle are referred to as the PZPM (*P*HD/*Z*n knuckle/*P*HD *m*otif) domain (50). This domain is conserved in Jade 1, 2, and 3, as well as in AF10 and the histone methyltransferase NSD1, both of which are associated with leukemia (50).

An activator role of BRPF proteins in MOZ/MORF complexes. In addition to the scaffold role, BRPF proteins are important for activating MOZ/MORF complexes, as reflected by upregulating the acetyltransferase activity and transcriptional activation potential of MOZ and MORF (Fig. 5 and 6). For nucleosomal histone H3 and free histones H3 and H4, BRPF1 stimulates the acetyltransferase activity of the MYST domains of MOZ and MORF (Fig. 5D and E). In addition, BRPF1 recruits ING5, which in turn increases the acetyltransferase activity further (Fig. 5D and E). This is very similar to what has been reported for the TIP60 and Esa1 complexes (20). Moreover, subunit interaction stimulates acetyltransferase activity and improves the substrate specificity of *Drosophila* Mof (41). Thus, it has emerged as a common theme that noncatalytic subunits regulate the acetyltransferase activity and substrate specificity of the MYST family of HATs.

Through its BN domain (see Fig. S3B in the supplemental material), BRPF1 binds to a flexible region within the MYST domain (see Fig. S2B and C in the supplemental material). Besides the BN1 and BN2 subdomains, domain M and perhaps the PHD finger region are required for BRPF1 to stimulate the HAT activity of MOZ (Fig. 5G). It is interesting to note that BRPF1 is acetylated by the MYST domain (Fig. 5E, G, and H). Intersubunit acetylation also occurs in the *Drosophila* Mof complex (4). It will be interesting to investigate whether and how BRPF1 acetylation may affect the function and regulation of MOZ/MORF acetyltransferase complexes.

For the stimulatory effects on the transcriptional activation of MOZ, the region from the bromodomain of BRPF1 to the C-terminal end of the PWWP domain is required for the reporters 6OSE2-Luc and OG2-Luc (Fig. 6B and C), but the BN domain is important for GM-CSF-Luc (Fig. 6D), suggesting that the domain requirement is dependent on the promoter

μg) and MOZ (0.05 μg) were cotransfected into HEK293 cells along with the same luciferase and β-galactosidase reporters as described for panel A. In addition, the expression plasmid for wild-type BRPF1 (0.1 μg) or its mutants at the amounts needed to achieve comparable expression levels shown in Fig. S5A in the supplemental material was cotransfected as indicated. Normalized luciferase activity from the transfection without any effectors was arbitrarily set to 1.0. Descriptions for panels C and D are the same as those for panel B except that the OG2-Luc and GM-CSF-Luc reporters were used as indicated. In panel D, 0.1 μg of the Runx1 expression plasmid was used instead of 0.05 μg of the Runx2 plasmid. (E) Schematic representation of BRPF1 and deletion mutants, with coactivation potential summarized at right.

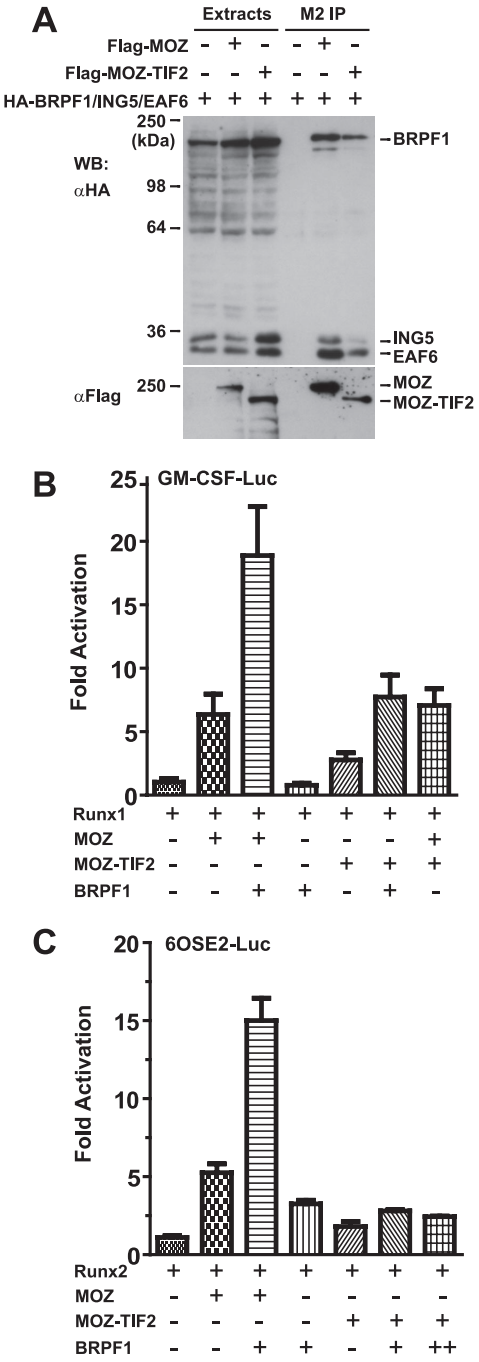

FIG. 7. Physical and functional interaction of MOZ-TIF2 with BRPF1. (A) The expression plasmid for Flag-tagged MOZ or MOZ-TIF2 was transfected into HEK293T cells along with those for HA-tagged BRPF1, ING5, and EAF6 as indicated. Extracts were prepared in buffer K150 for affinity purification on M2 agarose, and bound proteins were eluted with the Flag peptide for subsequent Western blotting (WB) with anti-HA and anti-Flag antibodies. Due to its low expression level, the amount of the MOZ-TIF2 expression plasmid used was three times as much as the MOZ plasmid. (B) The GM-CSF-Luc reporter and a β-galactosidase reporter were cotransfected into HEK293 cells along with expression plasmids for Runx1 (0.1 μg), BRPF1 (0.2 μg), MOZ (0.1 μg), and/or MOZ-TIF2 (0.6 μg). Luciferase activities were measured and normalized against β-galactosidase activities. Normalized luciferase activity from the transfection with Runx1 was arbitrarily set to 1.0. Description for panel C is the same as that for panel B but the 6OSE2-Luc reporter and the Runx2 expression plasmid were used.

context. While the inhibitory effects of ING5 on 6OSE2-Luc and OG2-Luc are puzzling (see Fig. S6A and B in the supplemental material) and contradict our previous observation (18), BRPF1 recruits ING5 for activation of the GM-CSF promoter (see Fig. S6C in the supplemental material). Further investigation is needed to determine the role of BRPF proteins, ING5, and EAF6 in activation of endogenous genes and to elucidate the underlying molecular mechanisms.

A key role of the MYST domain in complex formation and activation. Analysis of different deletion mutants revealed that the MYST domain is sufficient for complex formation (Fig. 3). Consistent with this, this domain is sufficient to promote tetrameric complex formation both in vivo and in vitro (Fig. 3A and 5A and B). More importantly, BRPF1 binds to this domain and stimulates its HAT activity (Fig. 5D and E). By itself, the MYST domain has minimal activity toward nucleosome substrates (11), but BRPF1 drastically stimulates this activity (Fig. 5E). Thus, the MYST domain of MOZ or MORF is sufficient for formation of functional acetyltransferase complexes, which is consistent with the fact that this is the only domain conserved in other members of the MYST family (1, 30, 51, 69).

Strikingly, BRPF1 association requires a very small region of the MYST domain (Fig. 3E and 8A). This region is highly conserved between MOZ and MORF but quite divergent among other MYST proteins (see Fig. S2B in the supplemental material). This region is unstructured and located right next to the catalytic center, so it may function as an "activation lid" to modulate the catalytic activity of MOZ and MORF (see Fig. S2C in the supplemental material) (24, 67). In comparison, MSL1 binds to the C2HC finger of MOF (41). This finger is opposite from the "activation lid" (see Fig. S2C in the supplemental material), so distinct activation mechanisms are used in different MYST complexes. Among known MYST complexes, HBO1 complexes are the most similar to those of MOZ and MORF (18), so it will be interesting to test whether the corresponding region of HBO1 plays a similar role. It will also be appealing to elucidate the molecular mechanism by which EPc proteins activate Esa1 and TIP60 (20).

Roles of PHD fingers in MOZ and MORF complexes. In addition to the MYST domain, MOZ and MORF possess PHD fingers and the SM domain (Fig. 8A). As the latter is known to function as a transcriptional activation domain (68), a remaining question is what roles the PHD fingers may play. Related to this, the PHD fingers of ING proteins recognize histone H3 methylated at lysine 4 (35, 45, 49, 54, 61). Consistent with this, only the ING-specific domain of ING5 is required for BRPF1 interaction (data not shown), suggesting that ING5 may target MOZ and MORF complexes to specific chromatin areas in a methylation-dependent manner. In support of this, ING5 recognizes lysine 4-methylated histone H3, and this modification makes histone H3 a better substrate for a reconstituted MORF complex (10). Whether the PHD fingers of MOZ, MORF, and BRPF proteins have similar functions is an interesting possibility awaiting further investigation. Alternatively, as recently reported for a yeast deacetylase complex (33), the PHD fingers may simply facilitate the recognition of nucleosome modifications by other protein modules. In this regard, the bromodomains and PWWP domains of BRPF1, -2, and -3 may be involved in recognition of acetylated and methylated histones, respectively (36, 42). Although further studies

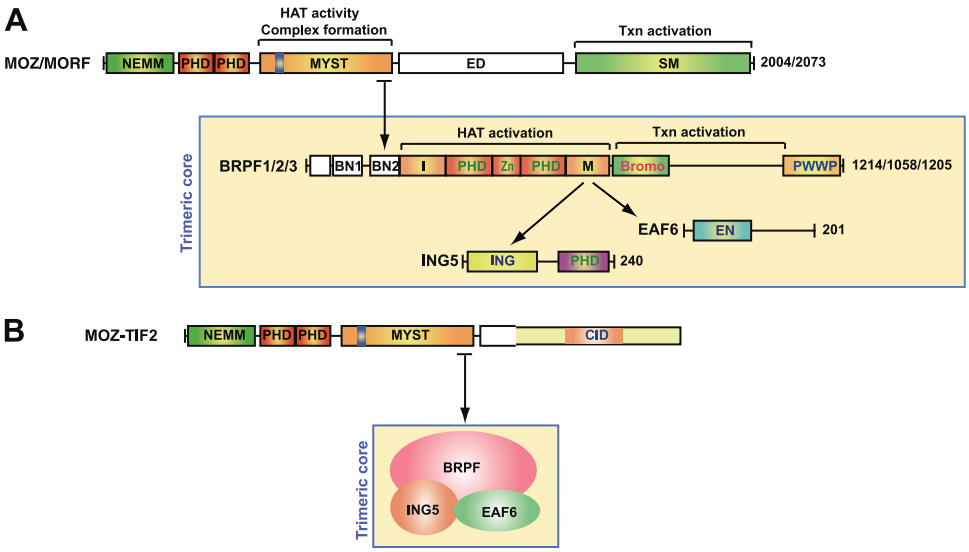

FIG. 8. (A) Schematic illustration of protein-protein interaction within MOZ and MORF complexes. A small region within the MYST domain of MOZ and MORF interacts with BRPF1 and paralogs, which utilize domain M for binding to ING5 and EAF6. ING5 and EAF6 form a trimeric core with BRPF1, -2, or -3. Association of ING5 with BRPF proteins promotes EAF6 interaction. The N-terminal domain of ING5 is sufficient for BRPF binding. The PHD fingers of ING5, BRPFs, MOZ, and MORF do not appear to be important for complex formation, but may mediate complex recruitment to specific chromatin domains (e.g., through histone H3 methylation). The bromodomains and PWWP domains of BRPF proteins may also recognize modified chromatin. The N-terminal domain of human EAF6 (GenBank accession no. NP_073593.2) is highly homologous to the counterpart in *Drosophila melanogaster* (sequence identity/similarity, 58/72%; GenBank accession no. NP_647981) but displays only limited similarity to the related protein in yeast (identity/similarity, 26/44%; GenBank accession no. NP_012615.1). Txn, transcription; EN, EAF6 N terminal. (B) Cartoon depicting recruitment of the BRPF/ING5/EAF6 trimeric core complex by leukemic MOZ-TIF2. CID, CBP/p300-interacting domain.

with chromatinized DNA templates are needed to examine these possibilities, it is clear that MOZ and MORF complexes possess various domains for different purposes (Fig. 8A). Related to this, different PHD fingers determine the substrate specificity of the HBO1 complexes (N. Saksouk, Y. Doyon, C. Cayrou, K. S. Champagne, M. Ullah, A. J. Landry, V. Cote, S. Tan, X. J. Yang, T. G. Kutateladze, and J. Cote, submitted for publication).

Molecular insights into related developmental and oncogenic processes. As the MYST domains of MOZ and MORF display no preference to BRPF1, BRPF2, and BRPF3 in vitro (Fig. 5A to B; see Fig. S2A in the supplemental material), these two HATs are likely to form tetrameric complexes with all three BRPF proteins in vivo. This suggests that MOZ and MORF are functionally homologous at least at the molecular level. Consistent with this, MOZ and MORF fusion proteins resulting from leukemia-associated translocations lead to a similar outcome (68). On the other hand, genetic analysis of MOZ and MORF in mice and zebrafish revealed that these two acetyltransferases play distinct roles in hematopoiesis, skeletogenesis, and neurogenesis (16, 26, 38, 39, 62, 64). This is perhaps due to their differences in spatiotemporal expression and regulation by posttranslational modification. Alternatively, full-length MOZ and MORF might form complexes differently from the catalytic domains analyzed herein. Further investigation is needed to address these important issues, but it is very likely that, as shown for p300 and CBP (as well as for GCN5 and PCAF), MOZ and MORF have overlapping as well as distinct roles in development.

The noncatalytic subunits affect the roles that MOZ and MORF play in vivo. Zebrafish BRPF1 is important for craniofacial development (31). Related to this, the *C. elegans* BRPF protein, Lin-49 (see Fig. S3A in the supplemental material), regulates different developmental programs (9, 13). *Drosophila* BPRF is homologous to BRPF1 (see Fig. S3A in the supplemental material). Thus, unlike MOZ and MORF, orthologs of BRPFs are present in *C. elegans* and *Drosophila melanogaster*. In addition, EAF6 is quite conserved from flies to humans. While the most similar ING protein in the worm (GenBank accession no. CAP23289) is still quite divergent from ING5 (identity/similarity, 24/42%), two *Drosophila* ING proteins are highly similar to ING5 (identities/similarities, 52/67% and 50/64%; GenBank accession no. NP_723814 and NP_609647, respectively). As domain M binds to ING5 and EAF6 (Fig. 4) and is evolutionarily conserved (see Fig. S3A in the supplemental material), orthologs of BRPF1, ING5, and EAF6 may form trimeric complexes in *Drosophila*, although this is less clear in *C. elegans*. The BN1 domain of BRPF1 is not conserved in dBRPF (see Fig. S3B in the supplemental material), so it will be interesting to determine if dBRPF binds Enok, the fly protein most related to MOZ and MORF (53).

The *MOZ* and *MORF* genes are rearranged in leukemia and leiomyomata (2, 6, 8, 29, 34, 40, 46, 69). Both MOZ and MORF are catalytic subunits of tetrameric complexes (18). BRPF1 and perhaps also BRPF2 and BRPF3 are crucial for the proper functioning of MOZ and MORF complexes in different tissues and developmental stages (Fig. 8A), so an interesting question is whether the noncatalytic subunits are subjects of chromosome abnormalities associated with leukemia and other types of cancer. As discussed above, the MYST

domain is sufficient for complex formation (Fig. 3), and this domain often remains intact in fusion proteins resulting from the leukemia-associated chromosome abnormalities (68), so complex formation should not be disrupted in related leukemia patients. This is the case at least for the MOZ-TIF2 fusion protein analyzed herein (Fig. 7A). As shown for BRPF1 (Fig. 7B), the noncatalytic subunits may modulate the oncogenic activity of leukemic fusion proteins involving MOZ and MORF (Fig. 8B). Thus, in addition to providing novel molecular insights for further investigation of how MOZ and MORF complexes are regulated, the current study sheds important light on how this pair of HATs and their associated subunits may be involved in regulating normal development and tumorgenesis.

ACKNOWLEDGMENTS

We thank Issay Kitabayashi, David M. Heery, Peter Cockerill, Yoshiaki Ito, Gerard Karsenty, and Stefano Stifani for kindly providing reporter and expression plasmids.

This work was supported by operating grants from the Canadian Institutes of Health Research (to J.C.) and the Canadian Cancer Society (to X.-J.Y.).

REFERENCES

1. **Avvakumov, N., and J. Côté.** 2007. Histone acetyltransferases of the MYST family and their roles in cancer. Oncogene **26:**5395–5407.
2. **Borrow, J., V. P. Stanton, Jr., J. M. Andresen, R. Becher, F. G. Behm, R. S. Chaganti, C. I. Civin, C. Disteche, I. Dube, A. M. Frischauf, D. Horsman, F. Mitelman, S. Volinia, A. E. Watmore, and D. E. Housman.** 1996. The translocation t(8;16)(p11;p13) of acute myeloid leukaemia fuses a putative acetyltransferase to the CREB-binding protein. Nat. Genet. **14:**33–41.
3. **Bristow, C. A., and P. Shore.** 2003. Transcriptional regulation of the human MIP-1alpha promoter by RUNX1 and MOZ. Nucleic Acids Res. **31:**2735–2744.
4. **Buscaino, A., T. Kocher, J. H. Kind, H. Holz, M. Taipale, K. Wagner, M. Wilm, and A. Akhtar.** 2003. MOF-regulated acetylation of MSL-3 in the *Drosophila* dosage compensation complex. Mol. Cell **11:**1265–1277.
5. **Candiano, G., M. Bruschi, L. Musante, L. Santucci, G. M. Ghiggeri, B. Carnemolla, P. Orecchia, L. Zardi, and P. G. Righetti.** 2004. Blue silver: a very sensitive colloidal Coomassie G-250 staining for proteome analysis. Electrophoresis **25:**1327–1333.
6. **Carapeti, M., R. C. Aguiar, J. M. Goldman, and N. C. Cross.** 1998. A novel fusion between MOZ and the nuclear receptor coactivator TIF2 in acute myeloid leukemia. Blood **91:**3127–3133.
7. **Carrozza, M. J., R. T. Utley, J. L. Workman, and J. Cote.** 2003. The diverse functions of histone acetyltransferase complexes. Trends Genet. **19:**321–329.
8. **Chaffanet, M., L. Gressin, C. Preudhomme, V. Soenen-Cornu, D. Birnbaum, and M. J. Pebusque.** 2000. MOZ is fused to p300 in an acute monocytic leukemia with t(8;22). Genes Chromosomes Cancer **28:**138–144.
9. **Chamberlin, H. M., and J. H. Thomas.** 2000. The bromodomain protein LIN-49 and trithorax-related protein LIN-59 affect development and gene expression in *Caenorhabditis elegans*. Development **127:**713–723.
10. **Champagne, K., N. Saksouk, P. Pena, K. M. Johnson, M. Ullah, X. J. Yang, J. Cote, and T. Kutateladze.** 2008. The crystal structure of the ING5 PHD finger in complex with an H3K4me3 histone peptide. Proteins **72:**1371–1376.
11. **Champagne, N., N. R. Bertos, N. Pelletier, A. H. Wang, M. Vezmar, Y. Yang, H. H. Heng, and X. J. Yang.** 1999. Identification of a human histone acetyltransferase related to monocytic leukemia zinc finger protein. J. Biol. Chem. **274:**28528–28536.
12. **Champagne, N., N. Pelletier, and X. J. Yang.** 2001. The monocytic leukemia zinc finger protein MOZ is a histone acetyltransferase. Oncogene **20:**404–409.
13. **Chang, S., R. J. Johnston, Jr., and O. Hobert.** 2003. A transcriptional regulatory cascade that controls left/right asymmetry in chemosensory neurons of *C. elegans*. Genes Dev. **17:**2123–2137.
14. **Cockerill, P. N., C. S. Osborne, A. G. Bert, and R. J. Grotto.** 1996. Regulation of GM-CSF gene transcription by core-binding factor. Cell Growth Differ. **7:**917–922.
15. **Cote, J., R. T. Utley, and J. L. Workman.** 1995. Basic analysis of transcription factor binding to nucleosomes. Methods Mol. Genet. **6:**108–128.
16. **Crump, J. G., M. E. Swartz, J. K. Eberhart, and C. B. Kimmel.** 2006. Moz-dependent Hox expression controls segment-specific fate maps of skeletal precursors in the face. Development **133:**2661–2669.
17. **Deguchi, K., P. M. Ayton, M. Carapeti, J. L. Kutok, C. S. Snyder, I. R. Williams, N. C. Cross, C. K. Glass, M. L. Cleary, and D. G. Gilliland.** 2003. MOZ-TIF2-induced acute myeloid leukemia requires the MOZ nucleosome binding motif and TIF2-mediated recruitment of CBP. Cancer Cell **3:**259–271.
18. **Doyon, Y., C. Cayrou, M. Ullah, A. J. Landry, V. Cote, W. Selleck, W. S. Lane, S. Tan, X. J. Yang, and J. Cote.** 2006. ING tumor suppressors are critical regulators of chromatin acetylation required for genome expression and perpetuation. Mol. Cell **21:**51–64.
19. **Doyon, Y., and J. Cote.** 2004. The highly conserved and multifunctional NuA4 HAT complex. Curr. Opin. Genet. Dev. **14:**147–154.
20. **Doyon, Y., W. Selleck, W. S. Lane, S. Tan, and J. Cote.** 2004. Structural and functional conservation of the NuA4 histone acetyltransferase complex from yeast to humans. Mol. Cell. Biol. **24:**1884–1896.
21. **Ducy, P., and G. Karsenty.** 1995. Two distinct osteoblast-specific *cis*-acting elements control expression of a mouse osteocalcin gene. Mol. Cell. Biol. **15:**1858–1869.
22. **Esteyries, S., C. Perot, J. Adelaide, M. Imbert, A. Lagarde, C. Pautas, S. Olschwang, D. Birnbaum, M. Chaffanet, and M. J. Mozziconacci.** 2008. NCOA3, a new fusion partner for MOZ/MYST3 in M5 acute myeloid leukemia. Leukemia **22:**663–665.
23. **Grégoire, S., and X. J. Yang.** 2005. Association with class IIa histone deacetylases upregulates the sumoylation of MEF2 transcription factors. Mol. Cell. Biol. **25:**2273–2282.
24. **Holbert, M. A., T. Sikorski, J. Carten, D. Snowflack, S. Hodawadekar, and R. Marmorstein.** 2007. The human monocytic leukemia zinc finger histone acetyltransferase domain contains DNA-binding activity implicated in chromatin targeting. J. Biol. Chem. **282:**36603–36613.
25. **Huntly, B. J., H. Shigematsu, K. Deguchi, B. H. Lee, S. Mizuno, N. Duclos, R. Rowan, S. Amaral, D. Curley, I. R. Williams, K. Akashi, and D. G. Gilliland.** 2004. MOZ-TIF2, but not BCR-ABL, confers properties of leukemic stem cells to committed murine hematopoietic progenitors. Cancer Cell **6:**587–596.
26. **Katsumoto, T., Y. Aikawa, A. Iwama, S. Ueda, H. Ichikawa, T. Ochiya, and I. Kitabayashi.** 2006. MOZ is essential for maintenance of hematopoietic stem cells. Genes Dev. **20:**1321–1330.
27. **Kindle, K. B., P. J. Troke, H. M. Collins, S. Matsuda, D. Bossi, C. Bellodi, E. Kalkhoven, P. Salomoni, P. G. Pelicci, S. Minucci, and D. M. Heery.** 2005. MOZ-TIF2 inhibits transcription by nuclear receptors and p53 by impairment of CBP function. Mol. Cell. Biol. **25:**988–1002.
28. **Kitabayashi, I., Y. Aikawa, L. A. Nguyen, A. Yokoyama, and M. Ohki.** 2001. Activation of AML1-mediated transcription by MOZ and inhibition by the MOZ-CBP fusion protein. EMBO J. **20:**7184–7196.
29. **Kitabayashi, I., Y. Aikawa, A. Yokoyama, F. Hosoda, M. Nagai, N. Kakazu, T. Abe, and M. Ohki.** 2001. Fusion of MOZ and p300 histone acetyltransferases in acute monocytic leukemia with a t(8;22)(p11;q13) chromosome translocation. Leukemia **15:**89–94.
30. **Lafon, A., C. S. Chang, E. M. Scott, S. J. Jacobson, and L. Pillus.** 2007. MYST opportunities for growth control: yeast genes illuminate human cancer gene functions. Oncogene **26:**5373–5384.
31. **Laue, K., S. Daujat, J. G. Crump, N. Plaster, H. H. Roehl, C. B. Kimmel, R. Schneider, and M. Hammerschmidt.** 2008. The multidomain protein Brpf1 binds histones and is required for Hox gene expression and segmental identity. Development **135:**1935–1946.
32. **Lee, K. K., and J. L. Workman.** 2007. Histone acetyltransferase complexes: one size doesn't fit all. Nat. Rev. Mol. Cell Biol. **8:**284–295.
33. **Li, B., M. Gogol, M. Carey, D. Lee, C. Seidel, and J. L. Workman.** 2007. Combined action of PHD and chromo domains directs the Rpd3S HDAC to transcribed chromatin. Science **316:**1050–1054.
34. **Liang, J., L. Prouty, B. J. Williams, M. A. Dayton, and K. L. Blanchard.** 1998. Acute mixed lineage leukemia with an inv(8)(p11q13) resulting in fusion of the genes for MOZ and TIF2. Blood **92:**2118–2122.
35. **Martin, D. G., D. E. Grimes, K. Baetz, and L. Howe.** 2006. Methylation of histone H3 mediates the association of the NuA3 histone acetyltransferase with chromatin. Mol. Cell. Biol. **26:**3018–3028.
36. **Maurer-Stroh, S., N. J. Dickens, L. Hughes-Davies, T. Kouzarides, F. Eisenhaber, and C. P. Ponting.** 2003. The Tudor domain 'Royal Family': Tudor, plant Agenet, Chromo, PWWP and MBT domains. Trends Biochem. Sci. **28:**69–74.
37. **McCullagh, P., T. Chaplin, J. Meerabux, D. Grenzelias, D. Lillington, R. Poulsom, A. Gregorini, V. Saha, and B. D. Young.** 1999. The cloning, mapping and expression of a novel gene, BRL, related to the AF10 leukaemia gene. Oncogene **18:**7442–7452.
38. **Merson, T. D., M. P. Dixon, C. Collin, R. L. Rietze, P. F. Bartlett, T. Thomas, and A. K. Voss.** 2006. The transcriptional coactivator Querkopf controls adult neurogenesis. J. Neurosci. **26:**11359–11370.
39. **Miller, C. T., L. Maves, and C. B. Kimmel.** 2004. moz regulates Hox expression and pharyngeal segmental identity in zebrafish. Development **131:**2443–2461.
40. **Moore, S. D., S. R. Herrick, T. A. Ince, M. S. Kleinman, P. D. Cin, C. C. Morton, and B. J. Quade.** 2004. Uterine leiomyomata with t(10;17) disrupt the histone acetyltransferase MORF. Cancer Res. **64:**5570–5577.
41. **Morales, V., T. Straub, M. F. Neumann, G. Mengus, A. Akhtar, and P. B.**

Becker. 2004. Functional integration of the histone acetyltransferase MOF into the dosage compensation complex. EMBO J. **23:**2258–2268.
42. **Mujtaba, S., L. Zeng, and M. M. Zhou.** 2007. Structure and acetyl-lysine recognition of the bromodomain. Oncogene **26:**5521–5527.
43. **Nagy, Z., and L. Tora.** 2007. Distinct GCN5/PCAF-containing complexes function as co-activators and are involved in transcription factor and global histone acetylation. Oncogene **26:**5341–5357.
44. **Ohta, K., M. Ohigashi, A. Naganawa, H. Ikeda, M. Sakai, J. Nishikawa, M. Imagawa, S. Osada, and T. Nishihara.** 2007. Histone acetyltransferase MOZ acts as a co-activator of Nrf2-MafK and induces tumour marker gene expression during hepatocarcinogenesis. Biochem. J. **402:**559–566.
45. **Palacios, A., P. Garcia, D. Padro, E. Lopez-Hernandez, I. Martin, and F. J. Blanco.** 2006. Solution structure and NMR characterization of the binding to methylated histone tails of the plant homeodomain finger of the tumour suppressor ING4. FEBS Lett. **580:**6903–6908.
46. **Panagopoulos, I., T. Fioretos, M. Isaksson, U. Samuelsson, R. Billstrom, B. Strombeck, F. Mitelman, and B. Johansson.** 2001. Fusion of the MORF and CBP genes in acute myeloid leukemia with the t(10;16)(q22;p13). Hum. Mol. Genet. **10:**395–404.
47. **Pelletier, N., N. Champagne, H. Lim, and X. J. Yang.** 2003. Expression, purification, and analysis of MOZ and MORF histone acetyltransferases. Methods **31:**24–32.
48. **Pelletier, N., N. Champagne, S. Stifani, and X. J. Yang.** 2002. MOZ and MORF histone acetyltransferases interact with the Runt-domain transcription factor Runx2. Oncogene **21:**2729–2740.
49. **Peña, P. V., F. Davrazou, X. Shi, K. L. Walter, V. V. Verkhusha, O. Gozani, R. Zhao, and T. G. Kutateladze.** 2006. Molecular mechanism of histone H3K4me3 recognition by plant homeodomain of ING2. Nature **442:**100–103.
50. **Perry, J.** 2006. The Epc-N domain: a predicted protein-protein interaction domain found in select chromatin associated proteins. BMC Genomics **7:**6.
51. **Rea, S., G. Xouri, and A. Akhtar.** 2007. Males absent on the first: from *Drosophila* to humans. Oncogene **26:**5385–5394.
52. **Reifsnyder, C., J. Lowell, A. Clarke, and L. Pillus.** 1996. Yeast SAS silencing genes and human genes associated with AML and HIV-1 Tat interactions are homologous with acetyltransferases. Nat. Genet. **14:**42–49.
53. **Scott, E. K., T. Lee, and L. Luo.** 2001. *enok* encodes a *Drosophila* putative histone acetyltransferase required for mushroom body neuroblast proliferation. Curr. Biol. **11:**99–104.
54. **Shi, X., T. Hong, K. L. Walter, M. Ewalt, E. Michishita, T. Hung, D. Carney, P. Pena, F. Lan, M. R. Kaadige, N. Lacoste, C. Cayrou, F. Davrazou, A. Saha, B. R. Cairns, D. E. Ayer, T. G. Kutateladze, Y. Shi, J. Cote, K. F. Chua, and O. Gozani.** 2006. ING2 PHD domain links histone H3 lysine 4 methylation to active gene repression. Nature **442:**96–99.
55. **Soliman, M. A., and K. Riabowol.** 2007. After a decade of study-ING, a PHD for a versatile family of proteins. Trends Biochem. Sci. **32:**509–519.
56. **Sterner, D. E., and S. L. Berger.** 2000. Acetylation of histones and transcription-related factors. Microbiol. Mol. Biol. Rev. **64:**435–459.
57. **Sun, Y., Y. Xu, K. Roy, and B. D. Price.** 2007. DNA damage-induced acetylation of lysine 3016 of ATM activates ATM kinase activity. Mol. Cell. Biol. **27:**8502–8509.
58. **Surapureddi, S., S. Yu, H. Bu, T. Hashimoto, A. V. Yeldandi, P. Kashireddy, M. Cherkaoui-Malki, C. Qi, Y. J. Zhu, M. S. Rao, and J. K. Reddy.** 2002. Identification of a transcriptionally active peroxisome proliferator-activated receptor alpha-interacting cofactor complex in rat liver and characterization of PRIC285 as a coactivator. Proc. Natl. Acad. Sci. USA **99:**11836–11841.
59. **Sykes, S. M., H. S. Mellert, M. A. Holbert, K. Li, R. Marmorstein, W. S. Lane, and S. B. McMahon.** 2006. Acetylation of the p53 DNA-binding domain regulates apoptosis induction. Mol. Cell **24:**841–851.
60. **Tang, Y., J. Luo, W. Zhang, and W. Gu.** 2006. Tip60-dependent acetylation of p53 modulates the decision between cell-cycle arrest and apoptosis. Mol. Cell **24:**827–839.
61. **Taverna, S. D., S. Ilin, R. S. Rogers, J. C. Tanny, H. Lavender, H. Li, L. Baker, J. Boyle, L. P. Blair, B. T. Chait, D. J. Patel, J. D. Aitchison, A. J. Tackett, and C. D. Allis.** 2006. Yng1 PHD finger binding to H3 trimethylated at K4 promotes NuA3 HAT activity at K14 of H3 and transcription at a subset of targeted ORFs. Mol. Cell **24:**785–796.
62. **Thomas, T., L. M. Corcoran, R. Gugasyan, M. P. Dixon, T. Brodnicki, S. L. Nutt, D. Metcalf, and A. K. Voss.** 2006. Monocytic leukemia zinc finger protein is essential for the development of long-term reconstituting hematopoietic stem cells. Genes Dev. **20:**1175–1186.
63. **Thomas, T., and A. K. Voss.** 2007. The diverse biological roles of MYST histone acetyltransferase family proteins. Cell Cycle **6:**696–704.
64. **Thomas, T., A. K. Voss, K. Chowdhury, and P. Gruss.** 2000. Querkopf, a MYST family histone acetyltransferase, is required for normal cerebral cortex development. Development **127:**2537–2548.
65. **Thompson, K. A., B. Wang, W. S. Argraves, F. G. Giancotti, D. P. Schranck, and E. Ruoslahti.** 1994. BR140, a novel zinc-finger protein with homology to the TAF250 subunit of TFIID. Biochem. Biophys. Res. Commun. **198:**1143–1152.
66. **Wang, A. H., M. J. Kruhlak, J. Wu, N. R. Bertos, M. Vezmar, B. I. Posner, D. P. Bazett-Jones, and X. J. Yang.** 2000. Regulation of histone deacetylase 4 by binding of 14-3-3 proteins. Mol. Cell. Biol. **20:**6904–6912.
67. **Yan, Y., N. A. Barlev, R. H. Haley, S. L. Berger, and R. Marmorstein.** 2000. Crystal structure of yeast Esa1 suggests a unified mechanism for catalysis and substrate binding by histone acetyltransferases. Mol. Cell **6:**1195–1205.
68. **Yang, X. J.** 2004. The diverse superfamily of lysine acetyltransferases and their roles in leukemia and other diseases. Nucleic Acids Res. **32:**959–976.
69. **Yang, X. J., and M. Ullah.** 2007. MOZ and MORF: two large MYSTic HATs in normal and cancer stem cells. Oncogene **26:**5408–5419.